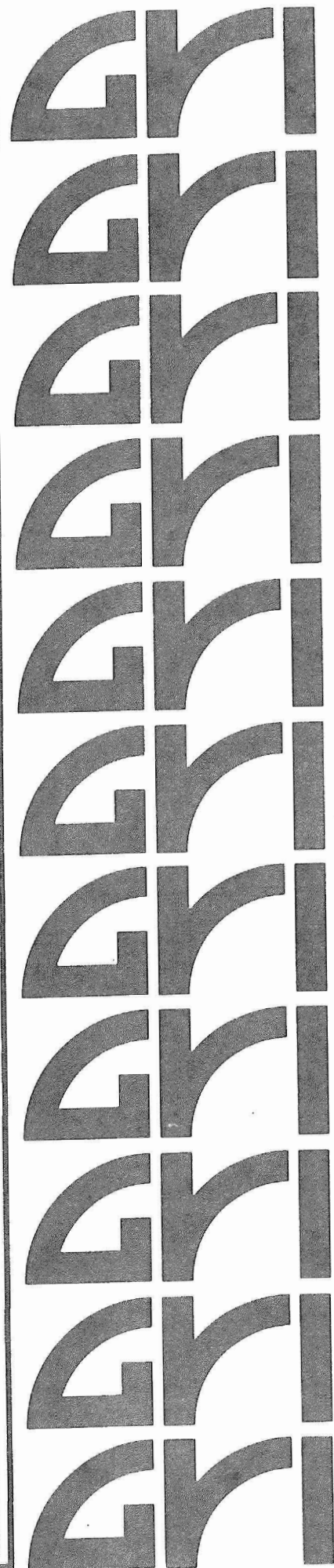


**QUANTIFYING RESERVOIR HETEROGENEITY  
THROUGH OUTCROP CHARACTERIZATION:  
2. ARCHITECTURE, LITHOLOGY, AND PERMEABILITY  
DISTRIBUTION OF A SEAWARD-STEPPING  
FLUVIAL-DELTAIC SEQUENCE,  
FERRON SANDSTONE (CRETACEOUS), CENTRAL UTAH**

**TOPICAL REPORT**  
**(November 1, 1989 – November 30, 1992)**

**Gas Research Institute  
8600 West Bryn Mawr Avenue  
Chicago, Illinois 60631**



QUANTIFYING RESERVOIR HETEROGENEITY THROUGH OUTCROP  
CHARACTERIZATION: 2. ARCHITECTURE, LITHOLOGY, AND PERMEABILITY DISTRIBUTION  
OF A SEAWARD-STEPPING FLUVIAL-DELTAIC SEQUENCE, FERRON SANDSTONE  
(CRETACEOUS), CENTRAL UTAH

TOPICAL REPORT

(November 1, 1989–November 30, 1992)

Prepared by

R. Stephen Fisher, Mark D. Barton, and Noel Tyler

Bureau of Economic Geology

W. L. Fisher, Director

The University of Texas at Austin

Austin, Texas 78713-7508

for

GAS RESEARCH INSTITUTE

Contract No. 5089-260-1902

GRI Project Manager, Anthony W. Gorody

July 1993

## DISCLAIMER

LEGAL NOTICE This report was prepared by the Bureau of Economic Geology as an account of work sponsored by the Gas Research Institute (GRI). Neither GRI, members of GRI, nor any person acting on behalf of either:

- a. Makes any warranty or representation, expressed or implied, with respect to the accuracy, completeness, or usefulness of the information contained in this report, or that the use of any apparatus, method, or process disclosed in this report may not infringe privately owned rights; or
- b. Assumes any liability with respect to the use of, or for damages resulting from the use of, any information, apparatus, method, or process disclosed in this report.

<b>REPORT DOCUMENTATION PAGE</b>	<b>1. REPORT NO.</b> GRI-93/0023	<b>2.</b>	<b>3. Recipient's Accession No.</b>
<b>4. Title and Subtitle</b> Quantifying Reservoir Heterogeneity through Outcrop Characterization: 2. Architecture, Lithology, and Permeability Distribution of a Seaward-Stepping Fluvial-Deltaic Sequence, Ferron Sandstone (Cretaceous), Central Utah			<b>5. Report Date</b> July 1993
<b>7. Author(s)</b> R. Stephen Fisher, Mark D. Barton, and Noel Tyler			<b>6.</b>
<b>9. Performing Organization Name and Address</b> Bureau of Economic Geology The University of Texas at Austin University Station, Box X Austin, Texas 78713-7508			<b>8. Performing Organization Rept. No.</b>
<b>12. Sponsoring Organization Name and Address</b> Gas Research Institute 8600 West Bryn Mawr Avenue Chicago, IL 60631 Project Manager: Anthony W. Gorody			<b>10. Project/Task/Work Unit No.</b>
			<b>11. Contract(C) or Grant(G) No.</b> (C) 5089-260-1902 (G)
			<b>13. Type of Report &amp; Period Covered</b> Topical Report 11/01/89-11/30/92
<b>15. Supplementary Notes</b>			<b>14.</b>
<b>16. Abstract (Limit: 200 words)</b>  The internal architecture of natural gas reservoirs fundamentally determines gas migration, production efficiency, and the volume of gas unrecovered at abandonment. To determine style and scale of reservoir complexity in fluvially dominated (seaward-stepping) deltaic reservoirs we investigated relations between sandstone architecture and permeability distribution in seaward-stepping deltaic Ferron genetic sequence (GS) 2 sandstone outcrops in central Utah. Distributary-channel, mouth-bar, and delta-front deposits are the volumetrically important sand repositories in the Ferron GS 2. Mouth-bar facies are laterally extensive and relatively simple sand bodies with moderate mean permeabilities. Distributary channels also have good permeability but are narrow, sinuous, and separated from mouth-bar sandstones by low-permeability bounding surfaces and thus they are difficult targets for development. Statistical analyses of permeability data show that lithofacies are the fundamental sandstone architectural elements. Therefore, lithofacies are the basic units that should be used to construct reservoir models. The variable preservation of lithofacies controls permeability throughout the system. Vertical and horizontal permeability correlation distances correspond to distances between bounding surfaces and to macroform dimensions. Estimates based on field-scale mapping show that 91 percent of the reservoir area could be contacted at 320-acre well spacing. Sandstone architecture and permeability relations of the Ferron GS 2 are similar to those in Lake Creek (Wilcox Group, Texas Gulf Coast) reservoirs. This outcrop-reservoir comparison confirms that outcrop data are transferable to reservoirs.			
<b>17. Document Analysis a. Descriptors</b>  Ferron Sandstone, fluvial-deltaic reservoirs, permeability distribution, reservoir analog, sandstone architecture, Utah  <b>b. Identifiers/Open-Ended Terms</b>  permeability analysis on outcrop reservoir analogs, sandstone architecture in landward-stepping depositional setting, sequence stratigraphy controls on sandstone permeability  <b>c. COSATI Field/Group</b>			
<b>18. Availability Statement</b> Release Unlimited		<b>19. Security Class (This Report)</b> Unclassified	<b>21. No. of Pages</b> XX
		<b>20. Security Class (This Page)</b> Unclassified	<b>22. Price</b>

## RESEARCH SUMMARY

Title	Quantifying Reservoir Heterogeneity through Outcrop Characterization: 2. Architecture, Lithology, and Permeability Distribution of a Seaward-Stepping Fluvial-Deltaic Sequence, Ferron Sandstone (Cretaceous), Central Utah
Contractor	Bureau of Economic Geology, The University of Texas at Austin, GRI Contract No. 5089-260-1902, titled "Quantification of flow unit and bounding element properties and geometries, Ferron Sandstone, Utah: Implications for heterogeneity in Gulf Coast Tertiary deltaic reservoirs."
Principal Investigators	Noel Tyler, Mark A. Miller, Ken E. Gray
Objectives	<p>We investigated outcrop exposures of the Ferron Sandstone (Cretaceous, central Utah), to test two fundamental hypotheses regarding sandstone architecture and the resulting controls on natural-gas reservoir properties. First, that depositional and diagenetic processes acting within a sequence stratigraphic framework produce a predictable arrangement of high- and low-permeability strata and consequently a predictable arrangement of flow units and barriers or baffles to natural gas migration. Second, that realistic three-dimensional reservoir models can be developed from knowledge gained at the outcrop and can be used to guide infill drilling and thereby optimize incremental gas reserve growth from mature sandstone reservoirs.</p> <p>The three major objectives of this work are to: (1) investigate the geologic and petrographic factors that produce reservoir compartments (flow units) and bounding elements (seals) in sandstone reservoirs on the basis of outcrop characterization studies; (2) show that such information can be used to construct realistic reservoir models, which can be used to test the effects of various infill drilling strategies; and (3) establish general principles for outcrop studies that can be used by other researchers.</p>
Technical Perspective	<p>Reservoir architecture, the internal arrangement of reservoir elements, governs migration paths during natural gas production. Reservoir architecture is the product of the depositional and diagenetic processes that cause the reservoir to form. Therefore, if we better understand the origin and history of the reservoir, we will be able to better predict paths of gas migration. With greater understanding of reservoir fabric and its inherent control on the paths of gas flow, we can more efficiently target remaining, conventionally recoverable natural gas that is prevented from migrating to the well bore by intrareservoir seals or bounding surfaces. Furthermore, advanced recovery strategies that account for the internal compartmentalization of the reservoir can be designed and implemented. The predictability of reservoir and seal properties, therefore, composes the crux of the proposed research. Our study focused on outcrop analogs to fluvial-deltaic reservoirs because this reservoir class accounts for 64 percent of total production from Texas Gulf Coast reservoirs.</p> <p>There are two projected long-term benefits of the study. First, increased understanding of internal sandstone architecture and improved methods for quantifying heterogeneity will facilitate developing more effective strategies to reduce risk in the extended development of gas reservoirs. Second, targeting incremental gas resources in mature reservoirs will lead to extended recovery of a low-cost, low-risk resource.</p>

## Technical Approach

We selected the Ferron Sandstone outcrop as a reservoir analog because it is well exposed, the sequence stratigraphic setting is established, and the various Ferron genetic sequences were deposited in wave-modified to fluvially dominated deltaic settings analogous to major Gulf Coast gas reservoirs. This volume presents results of our analyses of fluvially dominated deltaic sandstones, as the companion report no. 1 addressed the wave-modified—and landward-stepping—deltaic reservoir analog. We chose specific outcrops of GS 2 for investigation on the basis of position in the facies tract, quality of exposure, and orientation relative to sediment transport direction. We first photographed cliff faces with a medium-format camera and mapped major sand-body and bounding-surface geometries on photomosaics. We then established positions for vertical transects at 50- to 100-ft spacings, described the vertical sections, and measured permeability at 12-, 6-, or 4-inch intervals. At selected sites we measured permeability on nested two-dimensional grids to establish vertical and horizontal correlation distances. Horizontal permeability transects and lateral correlation of vertical permeability profiles provide a second measure of lateral permeability continuity. We determined field-scale relations of sandstone architecture and permeability by geologic mapping between outcrop locations. We used various geostatistical methods to identify permeability groups, distribution types, and correlation distances.

In conjunction with the field permeability characterization, we collected representative samples of probable flow unit, baffle, and barrier strata for petrographic and petrophysical measurements. The detrital and authigenic composition of Ferron sandstones was determined by standard thin-section petrography, scanning electron microscopy assisted by energy-dispersive analysis, electron microprobe analysis, and X-ray diffraction for clay-mineral identification. Petrophysical measurements were conducted at the Earth Science Engineering Laboratory and evaluated at the Center for Petroleum and Geosystems Engineering. Those results are presented separately.

## Results

Distributary-channel, mouth-bar, and delta-front deposits are the volumetrically important sand repositories in fluvially dominated Ferron sandstones. Distributary channels have good permeability but are narrow, sinuous, poorly connected to each other, and separated from underlying mouth-bar and delta-front sandstones by low-permeability bounding surfaces. Distributary channels, therefore, would be difficult targets for development. Mouth-bar facies are the reservoir rock because they have moderate mean permeabilities and are laterally continuous at the between-well (320-acre) scale. These findings show that sandstone architecture is distinctly different between the fluvially dominated (seaward-stepping) GS 2 deltaic sandstones reported here and the wave-modified (landward-stepping) Ferron GS 5 sandstones. Consequently, both outcrop and reservoir characterization studies must be placed within a sequence stratigraphic framework that takes into account sandstone stacking patterns, the location of space for sediment deposition, and sediment preservation potential.

We find a strong and predictable relation between macroforms, sedimentary facies, and permeability. For this reason we consider lithofacies and macroforms to be the fundamental architectural building blocks of both sandstones and sandstone reservoir models. Permeability relations within lithofacies and macroforms are consistent throughout the facies tract. However, syndepositional erosion and truncation of earlier deposits significantly modifies both preservation of lithofacies and macroforms and the resulting permeability structure. Permeability characteristics and structure are scale dependent. Changes in permeability variance, distribution type, and correlation structure closely reflect geologic scales of heterogeneity. Statistical

tests show that stratal types or lithofacies display the highest degree of permeability stationarity. Permeability variation and patterns at higher levels of stratal organization reflect variation in the proportion and arrangement of lithofacies or stratal types. Permeability characteristics are transferable between localities within the facies tract but not between sequences. Thus, reservoir properties must be calibrated to rock type for each genetic sequence.

Diagenetic overprint is mild because the Ferron Sandstone was never heated significantly during burial. Consequently, both detrital and diagenetic mineralogy correlate well with depositional facies. Sandstone texture reflects primary grain packing and pore structure only slightly modified by mechanical compaction of ductile grains and precipitation of minor amounts of pore-filling cement.

The distribution of sandstone types and dimensions, the degree of internal sandstone organization, segregation of mud from sand within and between channel macroforms, sandstone mineralogy, and permeability structure of seaward-stepping fluvial-deltaic sandstones are sufficiently different from those of landward-stepping sandstones to allow each system to be identified on the basis of well logs and other conventional exploration tools. Using field-scale maps of the Ferron GS 2 sandstone as a model for infill drilling shows that 91 percent of the total potential reservoir rock would be contacted at 320-acre well spacing. However, distributary channels are unlikely to be intercepted by drilling at conventional well spacings and are also unlikely to be drained by wells in delta-front and mouth-bar deposits. Thus, distributary-channel sandstones are good targets for geologically directed infill drilling.

Sandstone geometry and permeability patterns of the Ferron GS 2 at outcrop are similar to those of the Lake Creek G-2 and G-4 reservoirs (Wilcox Group, Texas Gulf Coast). The findings of this study support our hypothesis that outcrop characterization studies, performed within a sequence stratigraphic framework, can significantly improve three-dimensional reservoir models and guide infill drilling efforts in known, mature natural gas fields.

## INTRODUCTION

### Purpose

The complex internal architecture of sandstone reservoirs fundamentally controls natural gas migration, recovery, and the ultimate volume of conventionally recoverable natural gas remaining in the ground at reservoir abandonment. Increasing natural gas recovery, particularly in mature reservoirs, requires an improved understanding of reservoir anatomy and the spatial distribution of petrophysical properties that control gas migration. With a greater knowledge of reservoir anatomy and its inherent control on gas migration paths, we can more efficiently target remaining, conventionally recoverable hydrocarbons that are now prevented from migrating to the well bore by intrareservoir seals or bounding surfaces.

Sandstone complexity results from the diverse physical, chemical, and geologic processes that act over time and space to transform unconsolidated sediment into a structured reservoir. Understanding the processes that establish sandstone architecture is essential before we can predict petrophysical heterogeneity and gas migration paths in a reservoir. Once this knowledge is developed, we can construct more realistic models of natural gas reservoirs in which the depositional and diagenetic attributes that control production behavior are represented. These models, based on detailed geologic, petrographic, sedimentologic, and sequence stratigraphic information, can then be used to quantify the spatial distribution of flow units and barriers and to test various scenarios for enhancing resource recovery.

This study addresses the predictability of flow units, baffles, and barriers to gas movement in sandstone reservoirs by combining geologic, petrographic, and permeability quantification with geostatistical analyses and laboratory measurements of petrophysical properties. Because it is impossible to determine the detailed internal distribution of reservoir elements in the subsurface with present technology, we chose to investigate sand-body geometry, the positions and continuity of bounding elements between major sand bodies, internal architecture of sandstones, and



permeability distribution on a reservoir analog at outcrop. We hypothesized that we can use outcrop studies and permeability measurements to characterize sandstone heterogeneity and develop a realistic model that captures the three-dimensional distribution of baffles and barriers to gas flow in a sandstone reservoir. Our main purpose was to develop better methods for predicting the spatial distribution of intrareservoir barriers to gas flow in fluvial-deltaic sandstones and to demonstrate that deterministic models for sandstone gas reservoirs can be constructed based on data collected at outcrop.

### Projected Benefits to Natural Gas Consumers

Successfully quantifying reservoir complexity through outcrop studies will allow exploration geologists and production engineers to generate detailed, quantitative, three-dimensional models that can be used to test the effects of various reservoir development scenarios on natural gas recovery in mature fields. Ultimately this will increase the recovery of a low-cost, low-risk resource that would otherwise be unavailable with current technology.

### Objectives and Approach

The principal goal of this study was to develop methods for quantifying and predicting styles and scales of sandstone heterogeneity and to conduct a preliminary assessment of how this information would affect infill drilling strategies in analog reservoirs. Our approach was to combine outcrop characterization, petrographic analyses, collection and geostatistical interpretation of permeability measurements, and collection of samples for petrophysical testing to interpret the dimensions and distributions of flow units, baffles, and barriers in a sandstone reservoir. The work was organized into five specific objectives.

1. Select an appropriate outcrop for the field study.—We chose the Cretaceous Ferron Sandstone of central Utah as our outcrop analog because (1) it represents deposition in a variety of wave-modified to fluvially dominated deltaic settings, (2) it is well exposed both parallel and

perpendicular to sediment transport direction, and (3) the tectonic and sequence stratigraphic settings are well known. The Ferron outcrop gives us access to a fluvial-deltaic sandstone that was deposited in a rapidly subsiding foreland basin. As described in a following section, the Ferron Sandstone contains both seaward-stepping (fluvially dominated) and landward-stepping (wave-modified) sequences. It does not, however, present all possible combinations of the tectonic and depositional variables displayed by fluvial-deltaic sandstones. Our selection of the Ferron Sandstone was guided by the knowledge that information gained from there would be immediately applicable to many Texas Gulf Coast gas reservoirs and that the tectonic and geologic settings of the Ferron were already well established.

2. Quantify the external dimensions and internal architecture of the principal sandstone units.—To establish the field-scale geometry of a fluvial-deltaic reservoir, we first mapped the three-dimensional extent of the major sandstone bodies. We quantified the reservoir-scale internal architecture by preparing detailed outcrop cross sections mapping the arrangement of high- and low-permeability strata, which we assume to be analogs of reservoir flow units and baffles or barriers, respectively.

3. Quantify the detrital and diagenetic mineralogy of the sandstones.—Sandstone reservoirs have a long and complex history from initial sediment deposition through burial, compaction, cementation, porosity generation and reduction, and gas emplacement. Clearly we cannot expect to understand and predict the distribution of reservoir architectural elements solely by studying depositional processes. Petrographic studies augment the outcrop characterization by resolving the relative importance of depositional and diagenetic processes on porosity and permeability.

4. Determine correlation distances for permeability data.—In order to construct a realistic reservoir model we must know both the population statistics and the spatial structure of petrophysical properties such as permeability. We addressed this issue by collecting air-permeability values along transects and within two-dimensional grids using a field minipermeameter. We analyzed the structure of the data by determining population statistics, frequency distributions, and spatial relations, such as vertical and horizontal correlation lengths.

5. Measure petrophysical properties under effective reservoir conditions.—Finding ways to transform outcrop, petrographic, and petrophysical data to effective reservoir properties was one goal of this integrated research program. Petrophysical properties of samples selected to represent probable flow units, barriers, and baffles were measured at The University of Texas Earth Science and Engineering Lab (ESEL). Analyses include properties related to one- and two-phase flow and both static and dynamic mechanical properties. Results of the effort to establish transform functions between outcrop data and effective reservoir properties are presented separately (Miller and others, 1993).

#### Applicability of Outcrop Measurements to Reservoirs

Developing quantitative reservoir models from outcrop data requires that outcrop measurements are unaffected by weathering or other surficial processes and that the permeability structure (mean, variance, and distribution type) of outcrop measurements reflects the permeability structure of reservoir rocks. In particular, spatial and frequency distributions of permeability, not necessarily absolute values, must be portable from outcrop to subsurface. In clastic sequences this has proven to be a reasonable and useful approximation. Previous studies demonstrated the general portability of outcrop observations to the shallow subsurface (Stalkup and Ebanks, 1986; Goggin, 1988; this study) and to reservoirs (Tomutsa and others, 1986; Kittridge and others, 1989). Diagenetic effects on reservoir properties also may be important and must be evaluated for each outcrop analog-reservoir system (van Veen, 1977; Weber, 1982, 1986). These studies generally found that permeability distribution type, coefficient of variation, and variogram range agree sufficiently between similar facies in outcrop and reservoir to be useful in understanding reservoir production behavior.

## Outcrop Analog: Ferron Sandstone, Central Utah

The Upper Cretaceous (Turonian) Ferron Sandstone member of the Mancos Shale (fig. 1) is one of several clastic wedges that were deposited along the western shoreline of the Interior Cretaceous Seaway. West of the seaway the mountainous Sevier orogenic belt was repeatedly thrust-faulted and uplifted throughout the Cretaceous (Armstrong, 1968). Erosion of Paleozoic strata and basement rocks provided vast quantities of siliciclastic sediment, which were transported eastward and deposited in a foreland basin. Subsidence rates in central Utah exceeded the rate of eustatic sea-level fall during Ferron deposition. Thus, accommodation space was always available and sediment preservation potential was high throughout the Turonian (Gardner, 1991; 1993).

Ryer (1981a, b; 1982, 1983) and Gardner (1991; 1993) recently summarized the depositional and tectonic history of the Ferron Sandstone; only a brief summary is presented here. The Ferron Sandstone is a Cretaceous fluvial-deltaic system that exposes a wide range of depositional facies from fluvial through deltaic, coastal plain, and marine. Ryer (1981a) subdivided the upper Ferron interval into seven discrete delta lobes (genetic sequences [GS] 1 through 7) that progress from seaward-stepping (GS 1 and 2) sandstones at the base to vertically stacked (GS 3 and 4) deposits in the middle and landward-stepping geometries (GS 5, 6, and 7) at the top (fig. 2). Each unit consists of a regressive-transgressive cycle that is bounded by time-significant marine flooding surfaces. Gardner (1991; 1993) showed that systematic and predictable changes in facies arrangement, sediment stacking pattern, and sediment distribution within the facies tract of each genetic sequence are related to stratigraphic position. This well-documented geologic framework allowed us to quickly focus on two depositional pulses of the Ferron deltaic system that encompass the styles and scales of heterogeneity present in many Gulf Coast fluvial-deltaic gas reservoirs: (1) the landward-stepping GS 5 and (2) the seaward-stepping GS 2. This report summarizes our work on the seaward-stepping, fluvially dominated Ferron GS 2 genetic sequence; results of our work on the wave-modified, landward stepping Ferron GS 5 are presented in a companion report (Fisher and others, 1993).

Western  
Utah

West

Western  
Colorado

East

Sevier Orogenic Belt

Foreland  
Basin

Cretaceous  
Seaway

Fox Hills  
sandstone

Paleozoic  
Strata

Emery  
Sandstone  
Member

Mesaverde  
Group

Blue Gate  
Shale Member

Mancos  
Shale

Niobrara Limestone

Dakota Sandstone

Tununk Shale Member

Ferron Sandstone Member

QA 14506

Figure 1. Regional cross section of Cretaceous stratigraphy, central Utah (after Armstrong, 1968).

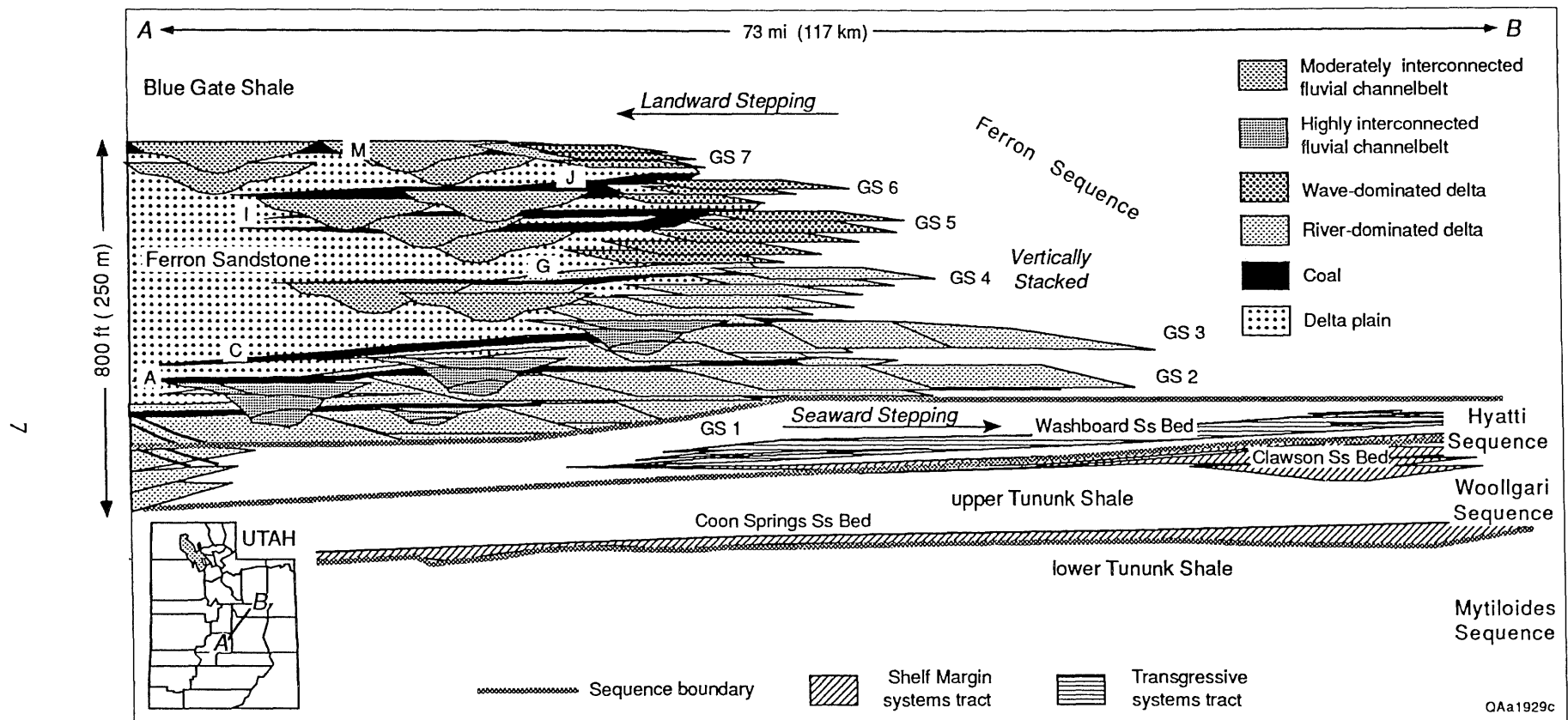


Figure 2. Schematic cross section depicting sequence stratigraphic relationships of the Ferron Sandstone in central Utah (after Gardner, 1992).

## REGIONAL SANDSTONE ARCHITECTURE

We studied the Ferron Sandstone outcrop to learn ways to predict the spatial arrangement of flow units (strata through which gas will readily pass) and barriers or baffles (strata that prevent, retard, or deflect gas flow) in reservoirs. Because accurate reservoir description is usually limited by insufficient knowledge of rock property distributions between wells, the usual approach is to stochastically model interwell reservoir architecture. However, we assert that the distribution of geologic heterogeneities is predictable if we understand the depositional and diagenetic processes that produce flow units, baffles, and barriers sufficiently well. Characterizing outcrop exposures is one way to quantify the spatial distribution of important reservoir elements with respect to geologic processes. The more realistic models developed from these studies can then be applied to actual reservoirs, appropriately conditioned by data specific to each reservoir.

Ferron GS 2 extends nearly 40 mi along depositional dip from the landward pinch-out of the delta-front facies near Willow Springs Canyon to the seaward extent near Dutch Flats (fig. 3). Internally, the sequence is composed of three parts: (1) a thin, basal transgressive unit consisting of an extensive but locally discontinuous bioturbated sandstone or siltstone, (2) a thick, regressive section composed of dominantly upward-coarsening prograding delta-front deposits, and (3) an aggradational section composed of thin delta-plain deposits and a complex network of thick, narrow distributary channels which locally erode and replace the progradational section (fig. 4).

### Transgressive Facies Tract

The transgressive base of GS 2 records marine flooding across the preexisting deltaic unit. In landward positions the facies is characterized by a sharp-based, mottled dark-gray and black, intensely bioturbated siltstone that contains abundant disseminated plant debris. Internal stratification is obscured by intense bioturbation. In more seaward positions a fossiliferous calcarenite with granules of chert and quartz, as well as fish and shark teeth, is present (Gardner, 1991). The marine flooding surface records an increase in the biological reworking of the sediment

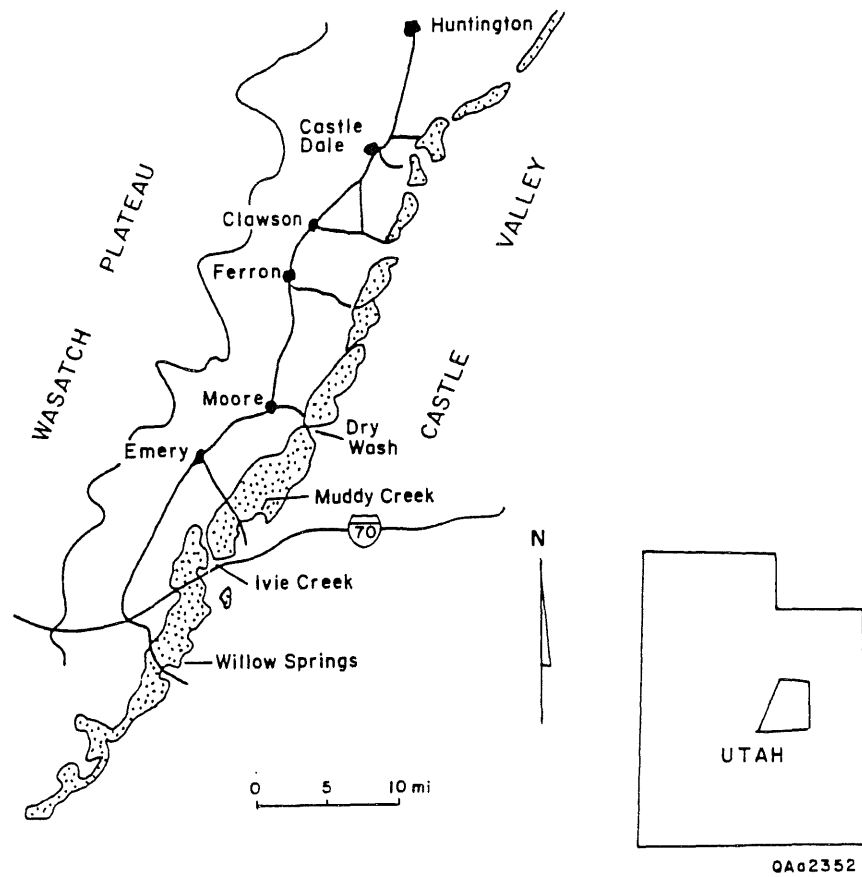


Figure 3. Location Ferron Sandstone outcrops in central Utah.



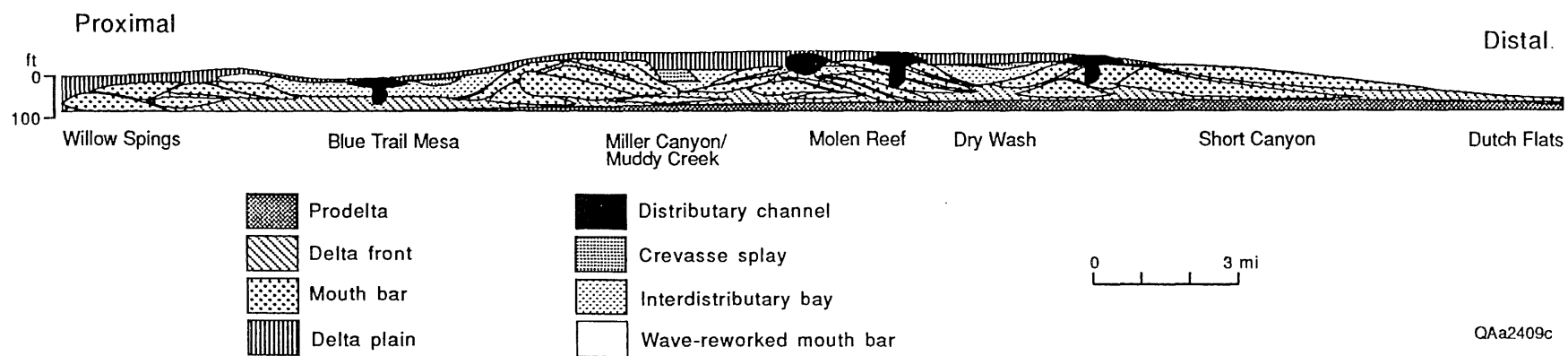


Figure 4. Ferron GS 2 facies architecture along depositional dip from landward to seaward extent.

and a decrease or cessation of deposition from landward sediment sources that occurred when the rate of relative sea-level rise was at a local maximum. During transgression, off-shore sedimentation on the shelf is minimal because sediments are trapped landward (Swift, 1968).

### Regressive–Shallow Marine Facies Tract

The regressive facies tract consists shallow marine sediments that display a high degree of facies variability. Deposits form a laterally extensive delta-front sand sheet that reflects the rapid progradation of the deltaic system over a broad platform. In the direction of progradation the delta front of GS 2 extends from its landward pinch-out in Willow Springs Wash northeastward to its seaward extent near the town of Clawson, a distance of approximately 40 mi. Deposits abruptly thicken in the vicinity of the landward pinch-out and gradually thin seaward (northeast) of Dry Wash, the seaward extent of distributary channel influence. Between Willow Springs and Dry Wash, thickness ranges from less than 60 ft in sand-poor regions (Blue Trail Canyon) to more than 120 ft in sand-rich regions such as Miller Canyon and Dry Wash.

In contrast to the delta-front facies of landward-stepping Ferron GS 5, which is dominated by storm processes, the delta front of GS 2 reflects the dominance of fluvial processes. Facies diversity is relatively high with a large proportion of preserved mud-rich lithologies. In a delta front dominated by fluvial processes the distributary mouth bar is the primary locus of sand deposition. A distributary mouth bar is a sandy shoal formed near the seaward limit of the distributary channel. Formation of the shoal is the result of the decrease in current velocity and carrying capacity of the stream as it leaves the channel. As the flow decelerates, the coarser sand fraction is deposited at the channel mouth and the fine-sand fraction is carried basinward in suspension. Continued progradation of the channel produces an elongate sand body that projects into the basin with the coarsest sand at its core and much finer grained deposits along the flanks. Typically, the delta-front section displays an upward-coarsening trend, as proximal mouth-bar, bar front, distal delta-front, and prodelta deposits are superposed during progradation.

Internally, mouth-bar deposits are characterized by multiple large-scale, inclined depositional surfaces that gently dip basinward. Bounding surfaces reflect the direction of mouth-bar progradation and develop on the bar front and flanks resulting from seasonal fluctuations in channel discharge. As the channel progrades basinward, effective hydraulic head is continually reduced and channel instability increases. Eventually, channel avulsion occurs as the distributary changes course to a portion of the delta plain offering a more favorable gradient. With channel avulsion and abandonment, the mouth bar subsides and may be subsequently reworked by marine processes. Overall progradational direction is seaward, but individual mouth bars and crevasse splay subdeltas may display divergent dip directions due to distributary-channel overextension and avulsion. In cross section, mouth-bar sands thin laterally over short distances and are bounded by finer grained prodelta, distal delta-front, bar flank, and interdistributary bay deposits.

Seaward on the delta slope, rapid sedimentation leads to gravitational instabilities and the generation of small to medium scale slope failure structures. The most important of these include slumps, slides, and growth faults. Where the delta-front surface is unstable because of oversteepening and undercompaction, slumps and slides commonly result. Such gravitational processes generate slide blocks, slump structures, convolute bedding, turbidites, and debris flows. Growth faulting results from sediment loading and episodic failure on the seaward side of the fault plane. Sedimentary units thicken across the fault as a result of syndepositional movement. This occurs particularly during deposition of denser sediment such as sand over less-dense mud and silt.

The cyclic nature of mouth bar evolution tends to severely compartmentalize the delta front sand sheet. Mouth-bar sandstones form a divergent but generally dip-oriented sandy framework. Internally, these deposits are composed of a series of discrete sidelapping and vertically stacked sandbodies separated from one another both laterally and vertically by fine-grained bar flank, interdistributary bay, and delta plain deposits (fig. 4).

Sand body arrangements or stacking patterns are largely controlled by rates of subsidence and marine reworking. Under conditions of rapid subsidence, upper mouth-bar sediments are moderately reworked by wave action and deposits are capped by fine-grained interdistributary-bay

deposits. Renewed progradation of a distributary channel across the foundered mouth bar results in vertically stacked sand bodies and sequences that may locally display several upward-shoaling sedimentary cycles. Under slower subsidence, more intense marine reworking may redistribute mouth-bar deposits into a series of small isolated barrier sand ridges or spits. These deposits are extremely clean and well sorted and interfinger laterally with fine-grained marsh and lagoon sediments. Locally, small tidal channels cross cut these deposits.

This process is illustrated near the landward pinch-out of the delta-front facies. At this location, distributaries prograde across a stable platform resulting from the deposition of the underlying genetic sequence. Subsidence into the underlying sediments is limited, and the resulting mouth-bar deposits sidelap each other laterally, are relatively thin (30–40 ft), and display a broad, flat geometry. Upper portions of the deposits are extensively reworked into an isolated, erosive-based, barrier island–ridge sand. In contrast, seaward of this position in the vicinity of Dry Wash, mouth-bar deposits sidelap one another laterally as observed at I-70, but also vertically stack, forming thick multiple upward-coarsening sequences. In addition, mouth-bar deposits are thicker (30–70 ft) than those observed at I-70. At Dry Wash, distributary channels have prograded beyond the underlying GS 1 and mouth-bar sands are deposited on unstable, undercompacted muds and silts. As a result, denser mouth-bar sands rapidly subside into the less-dense muds and silts. Resulting depressions may later be reoccupied by a distributary channel and renewed progradation across the foundered mouth-bar deposit may occur. This process results in the vertical stacking of deltaic lobes and sequences that may locally display several upward-shoaling sedimentary cycles. As this process continues, water depth and subsidence decrease and late-stage mouth-bar deposits are thinner than early stage mouth-bar deposits (~30 ft vs. 60 ft). The seaward increase in mouth bar thickness indicates a steepening of the shoreface profile during deltaic progradation. This trend towards a steepening shoreface profile is attributed to increased wave energy and/or increased rates of subsidence in the seaward direction.

## Aggradational–Delta-Plain Facies Tract

Capping most of the sequence is a thin veneer of delta-plain facies, including beach-barrier sand ridges, crevasse splay, marsh and swamp, and distributary-channel deposits. Distributary-channel deposits are superposed on the delta-front platform in a complex network of narrow, elongate distributary-channel fills that deeply incise and cross cut older delta-front and interdistributary-bay deposits and are laterally equivalent to the thin aggradational wedge that caps the progradational unit. Orientation of the channel sands is highly divergent and many times does not conform to orientation of underlying mouth-bar sands. Often, instead, well-preserved channel belts occupy fine-grained intermouth-bar regions such as shallow interdistributary bays. Such facies relationship indicates that channels are not directly related to adjacent mouth-bar deposits but instead are acting as conduits for the transport of sediment to more-basinward positions.

Attributes of the seaward-stepping distributary-channel belts suggest that they are strongly fluvially dominated. Externally, channels belts have isolated funnel-shaped geometries and poor connection with other channel belts. Channel belts display narrow, elongate geometries. Width–depth ratios are typically about ten. Internally, the channel belts consist of a series of vertical stacked, laterally restricted, highly amalgamated sand bodies that display a high degree of internal connectedness. The channel fill is sand rich and dominated by highly unidirectional trough cross strata separated by numerous thin sand-rich lag deposits.

## SANDSTONE ARCHITECTURE AND PERMEABILITY RELATIONS

A primary objective of this investigation is to determine the relationship of permeability correlation, structure, and scale dependence to sedimentary facies. Detailed facies analyses were conducted at the outcrop to identify potentially important lithofacies and bounding surfaces internal to discrete mappable sediment bodies, including the determination of lithofacies geometry, interconnectedness, and arrangement.

## Methods

Three-dimensional exposures of the Ferron Sandstone exist where canyons dissect the western limb of the San Rafael Swell, central Utah (fig. 3). Sparse vegetation and the absence of structural complexity allow continuous examination and sampling. We first selected outcrops for characterization on the basis of sequence stratigraphic setting, access, exposure, and safety. We then photographed the outcrop with a medium-format camera and compiled photomosaic panels for preliminary mapping of sand-body geometry and bounding element relations. Locations of vertical transects and grid sites were then selected for detailed analysis.

We established the relationship between permeability and lithofacies by calibrating permeability to facies, which are distinguished by common associations of sedimentary structures, grain size, and mineralogical composition. Because these parameters control permeability unless obscured by pervasive diagenetic modification, each lithofacies may be predicted to act consistently as either flow units or barriers throughout the genetic sequence. By comparing sedimentary attributes with permeability values, the influence of depositional and diagenetic processes on sandstone heterogeneity can be evaluated and the factors that control permeability variation most can be determined. We used three measures to characterize the relationship of permeability to sedimentary facies and lithofacies: (1) central tendency, (2) coefficient of variation, and (3) distribution type. The spatial correlation of permeability was estimated by comparing permeability profiles along the outcrop and by the semivariogram function. Because most of the sand in the seaward-stepping Ferron GS 2 resides in distributary-channel and delta-front-mouth-bar deposits, we concentrated on these facies.

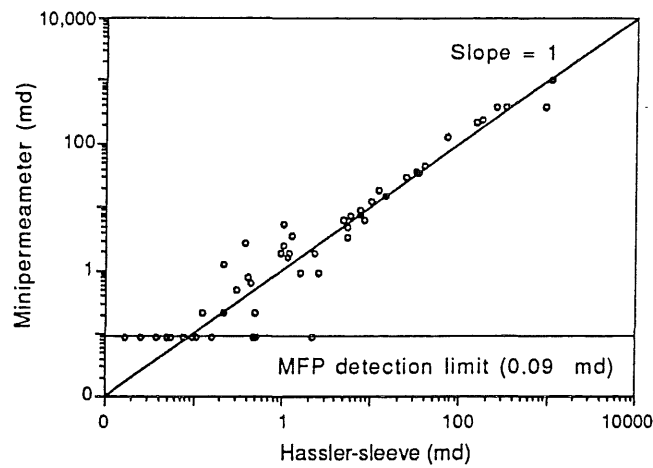
We measured permeability along vertical transects and at grid points with a portable minipermeameter. This gas-flow measuring device allows us to quickly make a large number of permeability determinations on the outcrop with minimal sample preparation. Numerous studies have demonstrated the accuracy of minipermeameter measurements in comparison with conventional measures of permeability (Weber, 1982; Goggin, 1988; Kittridge, 1988). In general, a

good correspondence between minipermeameter and conventional measurements is reported over the range of approximately one to several thousand millidarcys (md). Our minipermeameter has a detection limit of less than 0.1 md and can measure permeabilities as high as 2,500 md. Over the range of about 10 to 1,000 md, the minipermeameter gives the same values as the Hasseler-sleeve method (fig. 5). However, values below about 10 md tend to be slightly overestimated, whereas values greater than about 1,000 md are slightly underestimated. These discrepancies do not significantly affect our results. The intent of the outcrop characterization is to resolve the permeability structure within and between sand bodies. Other samples are collected for laboratory petrophysical measurements, which have greater accuracy and precision than field measurements.

Outcrop weathering effects are minimized by choosing relatively fresh surfaces and chipping away the outer surface of the rock. To evaluate the effects of surface weathering and sample site preparation, we compared permeability values determined from chipped sample sites with values measured on 2-inch-diameter cores taken from the same site. The similarity of values (fig. 6) indicates that permeability measured at the outcrop after chipping away the surface rind compares favorably with permeability within the outcrop.

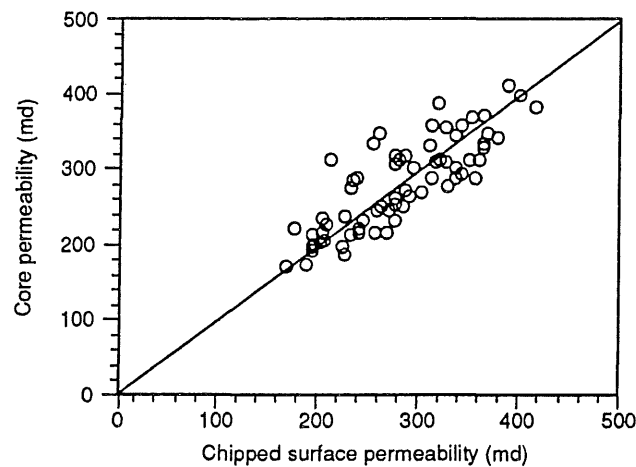
Data were collected along an extended outcrop of Ferron GS 2 near the I-70 roadcut (fig. 3). Sandstones and shales outcrop as 80- to 130-ft cliffs that extend from the roadcut east to northeast for approximately 1 mi. At this locality, GS 2 overlies Ferron GS 1 and is overlain by Ferron GS 3, with upper and lower boundaries of GS 2 marked by the sub-A and A coals, respectively. Delta-front deposits comprise most the section and display a high degree of facies variability. In the immediate vicinity of the road cut, thick mouth-bar sands directly overlie bar-flank deposits. Laterally to the northeast, mouth-bar sands thin and are replaced by fine-grained distal delta-front and interdistributary-bay deposits. Interrupting this sequence is a large distributary channel that locally deeply incises and replaces the adjacent delta-front deposits.

More than 5,000 permeability measurements were made on outcrops exposed near the I-70 road cut. Permeability was determined directly on the outcrop; data were collected in a fashion that would allow statistical analyses and determination of the population and spatial characteristics of



QA20052c

Figure 5. Comparison of minipermeameter- versus Hassler-sleeve-derived permeability. Miniper-meameter values are the average of measurements taken at each end of the core plug. Agreement is excellent for Hassler-sleeve values greater than 3 md.



QA20055c

Figure 6. Comparison of permeability measurements between cored and chipped surfaces.



permeability within lithofacies and facies assemblages. Descriptive attributes such as grain size, sedimentary structures, and sorting were recorded at each sample site. Data were collected at 6-inch intervals along a series of 50- to 250-ft-apart vertical transects. The sub-A coal was used as a stratigraphic datum with vertical transects extending to the top of GS 2. Lithologic attributes and discontinuities were correlated between vertical transects by direct inspection and their distribution was mapped on outcrop photomosaics. Permeability data were also collected from a sample grid within the distributary-channel facies and from a series of horizontal transects within the mouth-bar and bar-flank facies.

We characterized outcrop heterogeneity in a manner that reflects the origin, distribution, and scale dependence of genetically related strata and lithologic discontinuities. Within genetic units we quantified permeability and the spatial distribution of permeability patterns. Lithologic discontinuities (bounding elements) that define the dimensions of sandstone bodies typically have permeability values near or below the detection limit of our field equipment; for these units we recorded the dimensions, stratigraphic position, and lateral continuity of the elements.

Our sampling scheme allowed us to investigate both lateral and vertical permeability structure at various scales (table 1). At each sample site we measured air permeability and recorded depositional facies, lithofacies (rock type, facies, and bedding), grain size, fabric, and proximity to bounding elements. These data allowed us to relate permeability to geology and to thereby establish discrete permeability groups unique to a specific depositional and diagenetic setting. This information forms the basis for assigning values and distributions of petrophysical properties to reservoir sandstones from similar depositional settings.

We determined lateral and vertical permeability variation by correlating permeability profiles and by constructing semivariograms. Lithologic heterogeneities, such as shale breaks and other low-permeability intervals, are treated separately from the statistical analysis of sandstone permeability variation. We mapped the distribution of these elements on outcrop photomosaic panels and quantified their dimensions and density by probability distribution curves and other statistical techniques.

Table 1. Hierarchical sampling plan to provide material for outcrop characterization, petrographic, and petrophysical analyses.

Analysis Technique	Sample Set	Approximate number of Samples
Field minipermeameter	Genetic sequence Lithofacies Macroforms Facies Flow units Flow baffles Flow barriers Selected reservoir analogs	$N \times 10^5$
Petrographic composition	Genetic sequence Lithofacies Macroforms Facies Flow units Flow baffles Flow barriers Selected reservoir analogs	$N \times 10^2$
Petrophysical properties*	Flow units Flow baffles Selected reservoir analogs	$N \times 10^1$

\* Sample selection based on minipermeameter data and field relations.

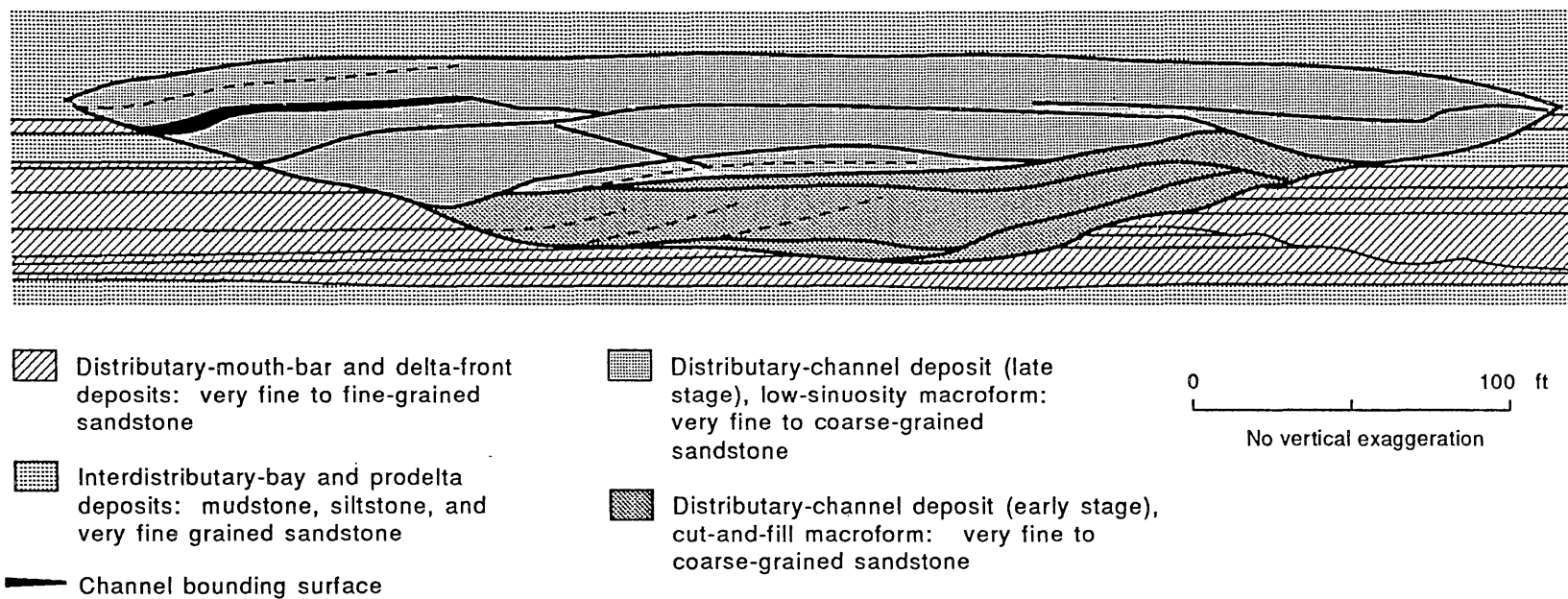
## Distributary-Channel Sandstones

### Architecture

Ferron GS 2 distributary channels form sandstone belts as much as 100 ft thick and 3,000 ft wide that are composed of multiple-channel sand bodies. Individual-channel sand bodies are 3 to 30 ft thick and tens to hundreds of feet wide. In profile they consist of an erosive-based, upward-fining to -coarsening sequence (Allen, 1965) that produces a compound bar form called a macroform (Jackson, 1976; Friend, 1983; Miall, 1985). In cross section, Ferron distributary-channel belts consist of laterally restricted highly amalgamated multistory macroforms at the base that grade into meandering, moderately amalgamated macroforms near the top.

We selected a large (500 ft wide and 70 ft thick) distributary-channel complex exposed along vertical cliffs where I-70 cuts through the Ferron Sandstone (fig. 7) for detailed examination. The complex is preserved as a narrow, elongate, ribbon sandstone, incised into fine-grained delta-front and distal mouth-bar deposits. Paleocurrent directions within the channel deposits are strongly unidirectional normal to the outcrop face. Internally, the channel is composed of a series of multistoried, highly amalgamated and interconnected macroform types, each of which shows a distinct stratal architecture. Macroform variability largely results from differences in channel morphology, macroform position within the channel, and channel development stage (Gardner, 1991).

Macroforms in the lower half of the channel are simple bar forms that have no large-scale accretion surfaces and contain a low diversity of sedimentary structures. They are characterized by 3- to 10-ft-thick, erosive-based, uniformly distributed medium- to coarse-grained sandstone sequences that consist of a sand-rich basal channel lag and crossbedded sandstone couplet. These erosive-based, lag-sandstone couplets stack to form a channel fill as much as 40 ft thick. The sand-rich nature of the channel lag results from the fixed channel position, with sand sourced from repeated erosion of underlying sand bodies. The low bedform diversity reflects erosional truncation by the overlying macroform and low preservation potential of a complete waning flow sequence.



QAa943(b)c

Figure 7. Facies architecture of distributary-channel sandstones.

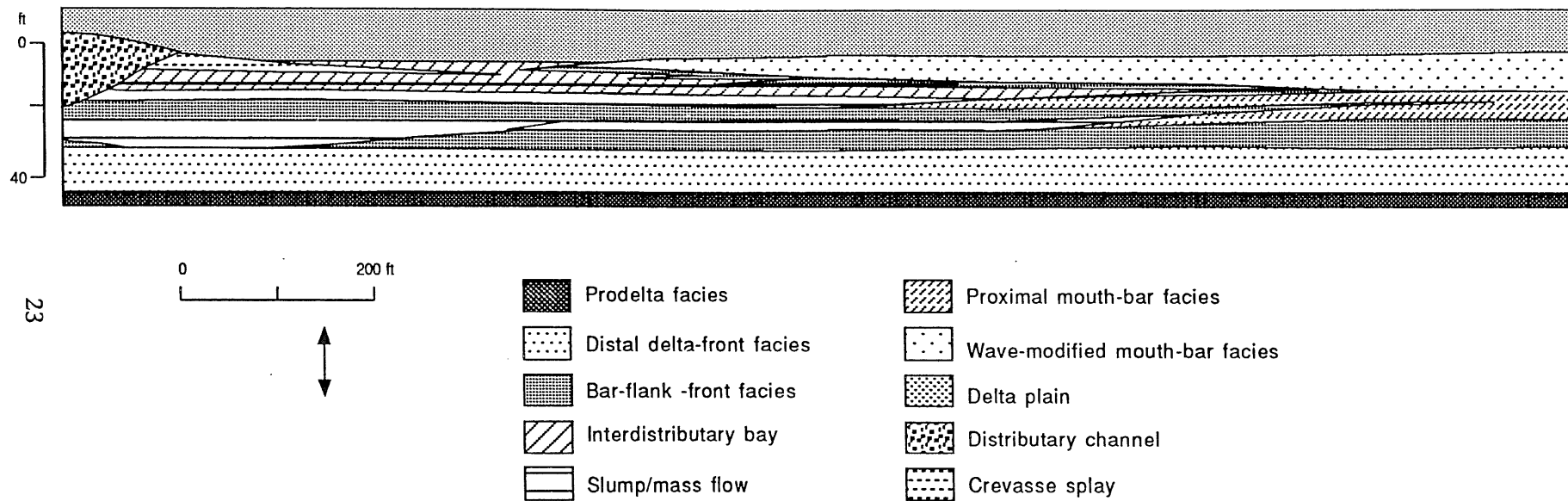
This cut-and-fill macroform represents extensive sediment reworking in a low-sinuosity, fixed channel.

Macroforms in the upper half of the channel display large-scale, low-angle, inclined accretion surfaces and contain suites of unidirectional bedforms that include ripple crossbedded, horizontal-inclined bedded, and trough crossbedded strata. Thin layers of silt and clay deposited during low-flow conditions may be preserved along the channel margin or accretion surface. Under higher flow conditions, underlying sediments were eroded or reworked and a heavy mineral lag developed along channel-base, accretion, and reactivation surfaces. This macroform records channel meandering within a fixed channel belt that produces a series of low- to high-sinuosity macroforms.

### Delta-Front Facies

#### Architecture

The I-70 outcrop provides a cross-sectional view through the progradational delta front and aggradational delta plain of GS 2, documenting lateral and vertical changes in facies architecture (fig. 8). In contrast to the delta-front facies of GS 5, which is a result of storm generated processes, the delta front of GS 2 is dominated by high-stage waning-flow events. Vertically, the delta front consists of an upward-coarsening sequence as prodelta, distal bar, bar front, and proximal mouth bar are superposed during progradation. Laterally, to the northeast, coarse mouth-bar sands thin and grade into bounding delta-margin and bar-flank deposits. Capping the strongly progradational sequence are deposits of the delta plain, including reworked mouth-bar sands, interdistributary-bay, crevasse splay, and marsh deposits. Facies characteristics are summarized in table 2. A detailed description of facies architecture and attributes follows.



QAa2410(b)c

Figure 8. Facies architecture of delta-front facies.

Table 2. Summary of lithofacies, occurrences, and permeability characteristics of Ferron GS 2 sandstones.

Lithofacies Group	Occurrence	Permeability Characteristics
Fine-grained to very coarse grained, poorly to moderately sorted, trough cross-stratified sandstone	Very common lithology, distributed throughout channel fill	Average = 204 md Range: 9 to 1,050 md Coefficient of variation = 0.81 Distribution: Log normal
Fine- to medium-grained, moderately sorted, horizontally stratified sandstone	Common lithology within accretion sets of low-sinuosity macroform type	Average = 85 md Range: 13 to 710 md Coefficient of variation = 1.05 Distribution: Log normal
Very fine grained to fine-grained, moderately sorted ripple-stratified sandstone	Deposited as final channel fill, common in low-sinuosity macroform type, uncommon in cut-and-fill macroform type	Average = 4.7 md Range: 0.09 to 13 md Coefficient of variation = 0.71 Distribution: Log normal
Medium-grained to very coarse grained, poorly sorted, sand-rich lag deposits with variable amounts of clay clast or siderite grains	Common lithology associated with lithologic discontinuities such as channel margins, accretion surfaces, and reactivation surfaces	Average = 38 md Range: 0.09 to 227 md Coefficient of variation = 1.15
Fine-grained sediments and organic laminated sandstone	Common lithology associated with accretion surfaces within low-sinuosity macroform type	Average = 2.6 md Range: 0.09 to 17 md Coefficient of variation = 1.67

### *Delta Platform—Prodelta and Distal Delta-Front Deposits*

The base of the sequence consists of a uniform interval of prodelta and distal delta-front mudstones, siltstones, and fine-grained sandstones that form a platform over which the mouth-bar and associated deposits advance. Prodelta deposits consist of a laterally extensive, sand-poor upward-coarsening interval of intercalated, argillaceous, fissile silty shale and nodular mudstone, interbedded with thin laminated to wavy-bedded siltstone and sandstone. Dark gray mudstones and silty shales contain disseminated very fine grained organic material. Bioturbation is sparse to moderate and best expressed on sandstone bedding planes. This facies represents normal marine deposition with minor amounts of low-energy wave action, or possibly turbidity currents along the lower delta slope during exceptional high stage conditions at distributary mouths (Elliot, 1986) and traction transport by storm-driven shelf currents from low-frequency, high-magnitude storms (Hunter and Clifton, 1982). Gradationally overlying the prodelta deposits is an upward-coarsening interval of thinly bedded silty fine sand to sandy silt. Although intense bioturbation is the dominant characteristic of this deposit, relict ripple laminations and hummocky cross stratification are preserved in places. This facies records a gradual decrease in water depth in a setting between storm and fair-weather wave base. Silt and sand transported by sediment gravity flows were efficiently reworked and redistributed by wave-generated storm currents and intense biological activity.

Overlying this interval are a diverse assemblage of sedimentary features, including slump and slide features, massive and thin graded beds exhibiting sharp bases and incomplete Bouma sequences, variable amounts of bioturbation, abundant ripple laminations, and hummocky cross stratification. Lateral shifts in the character of these deposits reflect the influence of diverse sedimentary processes.



### *Bar-Flank and Distal Mouth-Bar Deposits*

Bar-flank deposits define a transition from underlying prodelta mudstone and distal delta-front mudstone and muddy siltstone to overlying channel mouth-bar sandstone and record progradation of distributary mouth bars over the distal delta-front and prodelta deposits. The lower portions of the bar-flank deposits are dominated by a series of sediment gravity flows and related phenomena, which resulted in the progressive infilling of low-lying areas adjacent to the advancing distributary mouth-bar complex. The upper portion of this facies consists of a strongly aggrading turbidite wedge deposited along the margin of a prograding mouth-bar complex caused by density underflows related to high-stage fluvial events and deposition of fine-grained sediment from suspension.

The base of this interval consists of very fine to medium-grained sandstone, which is generally coarser grained than adjacent deposits. Units are broadly lenticular with maximum thicknesses of 15 ft and width-to-thickness ratios between 20 and 100. Sandstones are massive, homogeneous, ungraded to highly contorted, and may show dish structures. Lower boundaries are sharp and range from concave to flat or uneven. Deposits typically occur in the lower portion of the sequence-overlying prodelta, bioturbated delta-front, or turbidite deposits; often they form the base of an upward-shoaling sequence. Laterally, deposits are often stacked in an offset fashion separated by heterolithic turbidite deposits. Emplacement of the facies was probably by liquefied-sand flows, derived from the metastable slope of the advancing mouth-bar complex (Koning, 1982; Nemec and others, 1988).

In cross section, the upper bar-flank facies forms a wedge that thickens away from the mouth-bar complex. Internally, the interval consists of a series of large-scale, low-angle, concave, upward-inclined bedding planes of interbedded sandstone as much as 3 ft thick, and inch-thick mudstone interbeds that progressively thin and dip away from the advancing mouth-bar complex. Beds offlap in a succession that displays a well-developed upward bed-thickening and -coarsening trend. Inclined sandstone beds are characterized by a low-angle top-truncated upper surface that decreases

in inclination downward, where it interfingers with mudstone interbeds. Sedimentary structures within a downdip transect of an individual bed record progressively decreasing flow velocities, grading laterally from massive and parallel bedded sands at the proximal portions to ripple laminated and bioturbated structures at the distal portions. Internally, sandstone beds contain horizontal laminations with low-amplitude erosional bases. The horizontally laminated sandstones grade upward to wavy laminations that are overlain by thin cosets of asymmetrical ripples. Down depositional dip, the erosive basal contact of the amalgamated sandstone beds grades to a depositional surface characterized by a broad low-amplitude surface that is draped by wavy laminations. Bedding planes in this interval contain wood fragments and abundant, very fine grained disseminated organic matter. At their distal portions, beds gradually thin and downlap older deposits, while at their proximal portions individual beds thicken and abruptly terminate against trough cross-stratified mouth-bar sands. Lateral extent of the beds varies from several hundred feet to several thousand feet. Mudstone beds are 1 to 4 inches thick, laminated, contain abundant disseminated plant debris that may form discrete carbonaceous-rich intervals, and are sparsely bioturbated. Laterally in the direction of accretion, mudstone interbeds increase in thickness and frequency near the base and pinch out upward against sandstone beds that are increasingly thick toward the top. The sequence is capped by flat-based erosive sandstone that displays 1- to 4-ft-thick amalgamated, unidirectional trough cross strata.

The large-scale, inclined depositional surfaces record progradation of the bar-front and bar-flank facies. The change in internal stratification of an inclined bed down depositional dip provides evidence for sediment transport by decelerating flow in a bottom-hugging current. Multiple higher energy sediment gravity flows down the dipping depositional surface resulted in upper planebed conditions that produced the erosive-based, laminated sandstones. This was followed by multiple waning-flow events that record a progressive decrease in flow strength from upper planebed to lower flow-regime conditions with superimposed ripple laminations reflecting traction and rapid fallout. The upper fine grained interval capping the succession records gradual settling of very fine grained material from suspension. Bioturbation is sparse, occasionally occurring along the upper

surfaces of the sandstone beds. This style of deposition likely developed during seasonal flooding events.

Laterally in a northeast direction along the face of the outcrop, the bar-flank facies gradationally thins and fines from proximal mouth-bar deposits into distal-bar deposits, which display a mix of both storm- or wave-generated, high-stage waning-flow events. Deposits consist of silty fine sand to sandy silt, characterized by an upward-coarsening sequence of thinly interbedded sandstone, siltstone, and mudstone. Sandstone beds are sharp to erosive based and 2 to 5 inches thick; they contain waning-flow sequences that grade from massive to planar laminations at the base, to wavy laminations and hummocky cross stratification at the top. Sandstone beds are commonly capped by sets of asymmetrical and symmetrical ripples. Bioturbation is sparse to moderate, with echinoid trails and feeding trails of *planolites*, *skolithos*, and *thalassinoides* on bedding planes. This facies records a gradual decrease in water depth in a setting between storm and fair-weather wave base. Mudstone interbeds provide evidence of suspension deposition during normal fair-weather conditions, whereas sandstone beds record episodic waning-flow events from exceptional distributary floods and storms. During progradation of the delta, sand was episodically transported by sediment gravity flows from increasingly effective distributary floods. These deposits were reworked and redistributed by wave- and wind-generated storm currents (Swift, 1968).

#### *Proximal Mouth-Bar Deposits*

The bar flank facies is capped by flat based erosive sandstone that displays 20- to 45-inch-thick amalgamated, unidirectional trough cross strata. These deposits comprise the highest energy shoal water deposits of the mouth-bar sequence. This facies is well exposed along the west side of the I-70 road cut. Northeast along the face of the outcrop these deposits thin dramatically and interfinger with fine-grained distal mouth-bar and interdistributary-bay deposits. The interval consists of massive to thick-bedded, clean, well-sorted sands containing trough cross strata and dewatering structures. The uppermost deposits may display planar horizontal stratification and

scour and fill structures near the proximal portions. To the southwest, deposits laterally thicken into a lenticular channel fill that deeply erodes into underlying inclined beds. This facies is attributed to unidirectional sand waves that descended down the bar face from fluvially induced traction currents at the distributary mouth. The upper portion near the proximal extent may display numerous reactivation surfaces and scour and fill structures that reflect processes active at the distributary mouth, including shallow channelization of flow, redistribution and reworking of sediment by wave currents, and seasonal fluctuations in river discharge.

#### *Wave-Modified Mouth-Bar Sands*

Upper distributary mouth-bar sediments may be redistributed by wave activity into several types of sand bodies including mature beach or barrier island sand bodies. Deposits are closely associated with mouth-bar deposits and are similar in character to bar-crest facies. Unlike the bar-crest deposits, however, barrier island-ridge sands are separated from mouth-bar deposits by fine-grained lagoon and interdistributary-bay deposits. Sandstone is composed of extremely clean, well-sorted, medium-grained sand. Foreshore deposits display multidirectional trough cross bedding and plane horizontal stratification. Bedding plane discontinuities display a distinct seaward dip. Laterally, these deposits may be replaced by erosive tidal channel or tidal inlet deposits and may thin away from the mouth-bar complex and interfinger with interdistributary-bay and -marsh deposits. Upper surfaces are often bioturbated or rooted and overlain by carbonaceous rich marsh or back-swamp deposits.

#### *Interdistributary-Bay Fill and Crevasse Splay*

Well developed interdistributary-bay fill deposits cap delta-front platform deposits and sidelap amalgamated distributary mouth-bar facies. These rocks consist of interbedded upward-coarsening gray-brown mudstone, siltstone, and fine-grained sandstone. Sandstones display interference ripple

bedforms. Bedding surfaces often display articulated plant fossils. Diagenetic iron carbonate forms thin persistent bands and large lenticular concretions.

#### *Back-Swamp-Marsh*

These rocks are essentially claystones with minor amounts of siltstone; they are commonly evenly and horizontally bedded or have mild wavy irregular bedding. This facies contains much carbonaceous plant debris and some rootlets and burrows. It grades into underlying deposits, which are in most cases upper mouth-bar or distributary-channel deposits.

#### Sand Body Dimensions

One task of this project is to collect quantitative geologic information on the geometry and distribution of specific sandstone bodies. The focus of the study is on the dimensions of key reservoir facies. These include distributary-channel and mouth-bar deposits within a single progradational event of a fluvially dominated deltaic sequence. The dimensions of the sand bodies of interest are maximum thickness and width and, where available, maximum length. Data on mouth-bar deposits were obtained primarily from two main outcrop areas within GS 2. The study areas chosen were a series of canyons in the vicinity of the I-70 road cut and Dry Wash (fig. 3). Measurements on channel sand bodies were made from a variety of locations along the outcrop belt of GS 2.

Typically, channel belts display a broad funnel-shaped geometry and internally are composed of a series of vertically stacked channel forms. Figure 9 provides a summary of width-to-thickness relationships for distributary-channel belts in GS 2. Most distributary-channel belts are 300 to 700 ft wide; the average channel belt is approximately 600 ft wide. Channel belt thickness varies from 33 to 75 ft, averaging 55 ft. Based on this sample set, the value of ten appears to be a good representation of width-to-thickness ratios for these channel belts. Channel belt length was more difficult to estimate but at least one channel belt could be traced more than 4 mi. Channel-form

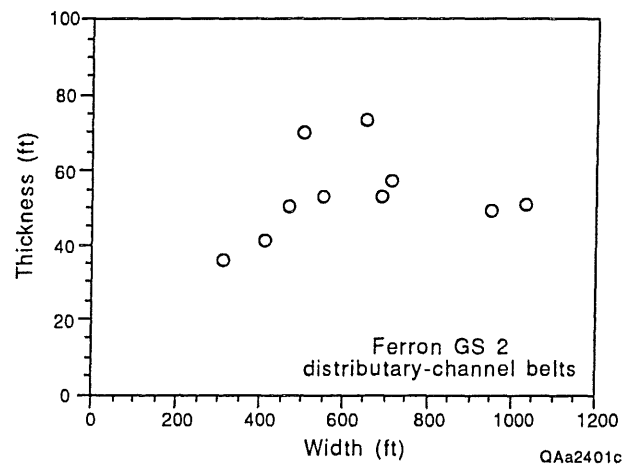


Figure 9. Distributary-channel dimensions (width/thickness).

thickness varied from several feet to tens of feet, with widths ranging from tens of feet to hundreds of feet. Width-to-thickness relations are shown in figure 10 for macroforms in a channel belt at I-70, which was composed of 10 distinct channel forms.

Figure 11 summarizes descriptive statistics on width-to-thickness ratios for GS 2 distributary mouth-bar deposits. Mouth-bar deposits displayed considerable variation in thickness, ranging from less than 20 ft to more than 60 ft. Widths also displayed considerable variation, ranging from about 1,000 to 9,000 ft. As previously discussed, two populations exist: (1) thinner mouth-bar deposits that formed in shallow water near the landward pinch-out of the delta-front facies and (2) mouth-bar deposits that formed in deeper water and more seaward positions.

Near the I-70 road cut, sand bodies within the regressive and aggradational portions of GS 2 were mapped over an area of approximately 14 mi<sup>2</sup> (fig. 12a, b). Distributary-channel belts are preserved as narrow elongate sand bodies that externally display a very low degree of connectivity with other channel belts. Despite this characteristic, the cross-cutting nature of these deposits to adjacent delta-front deposits indicates that they are likely to have an important impact on fluid flow, possibly acting as conduits between laterally adjacent but compartmentalized mouth-bar deposits. Channel belt orientation approximately parallels the direction of deltaic progradation, but significant departures from this trend are observed. In most cases the position of channel sand bodies does not conform to the orientation of underlying mouth-bar sands. Comparison of channel belt distribution to the distribution of contemporaneous sand bodies indicates that channel belts are often located within mud-rich intermouth-bar areas. Such regions likely existed as topographic lows and thus were a preferred site for channel belt migration. Although dimensions of individual distributary-channel belts are substantial, overall they comprise less than 5 percent of the total GS 2 sediment. Thus, the probability of contacting one of these sand body types by conventional drilling strategies is relatively low.

Distributary mouth-bar deposits are the dominant preserved GS 2 sand body type. These deposits extend over 30 percent of the I-70 study area. In plane view, these deposits combine to form lobate to elongate sand bodies that roughly parallel the dominant progradational direction. At

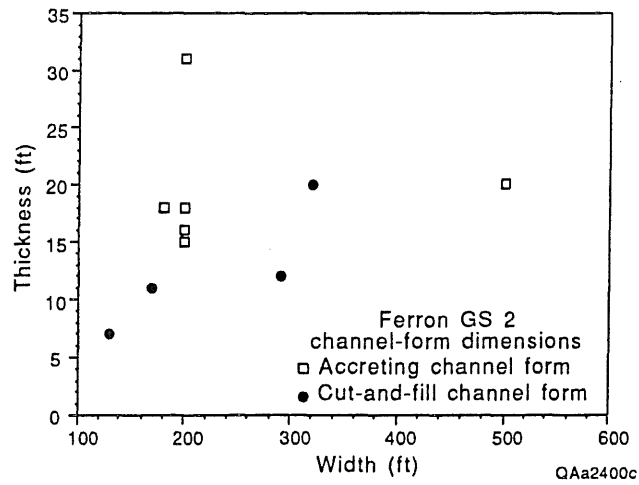


Figure 10. Distributary-channel-form dimensions (width/thickness).

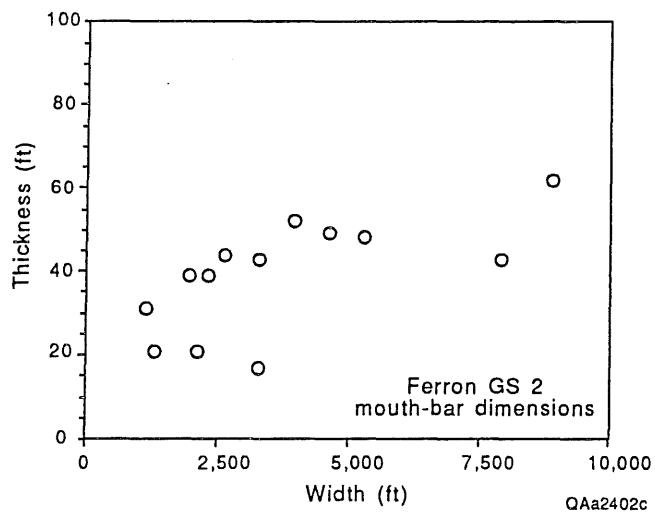


Figure 11. Distributary mouth-bar dimensions (width/thickness).



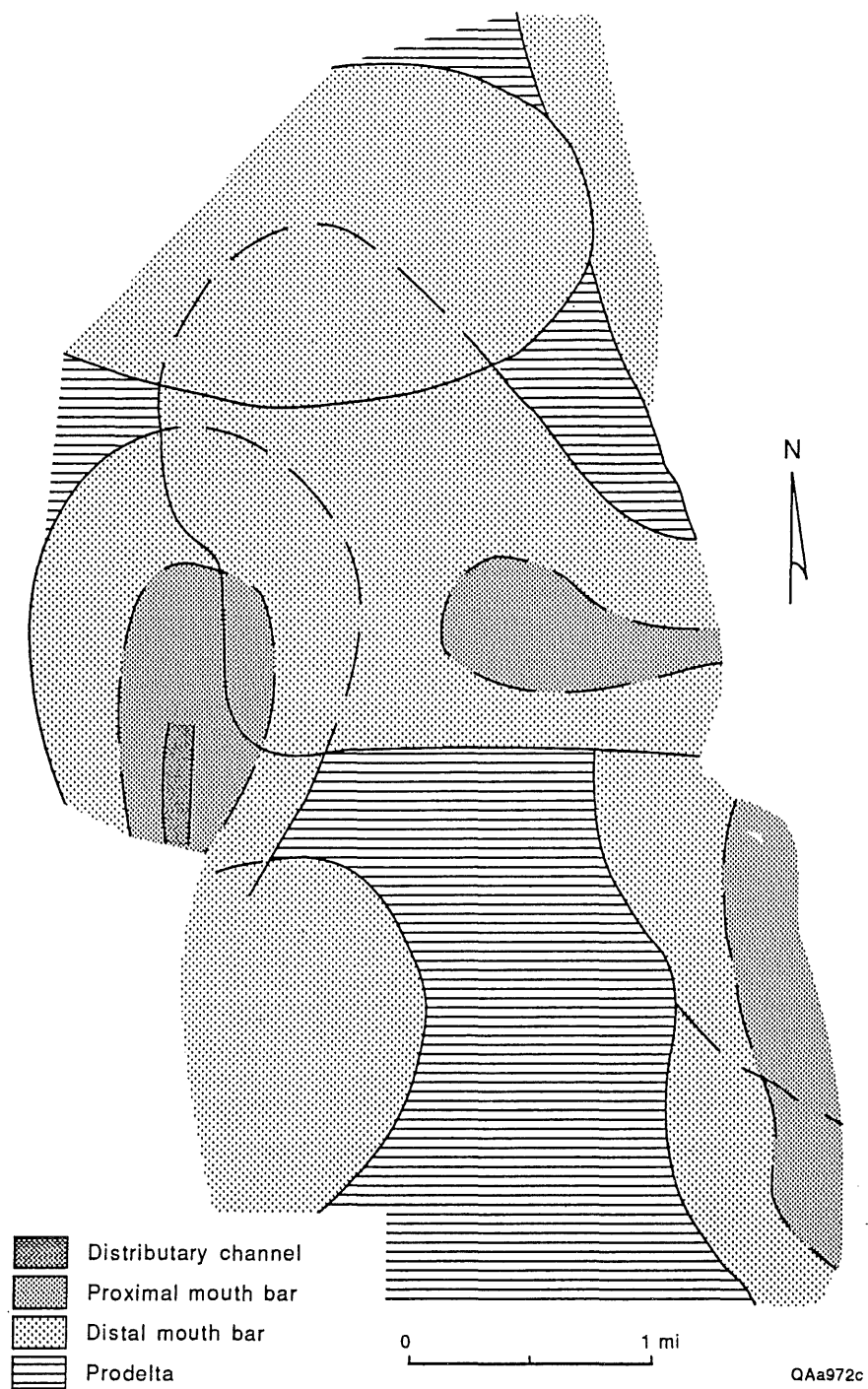


Figure 12. (a) Map of facies architecture in regressive Ferron GS 2.

## Ferron GS 2 (upper) Distributary Aggradation

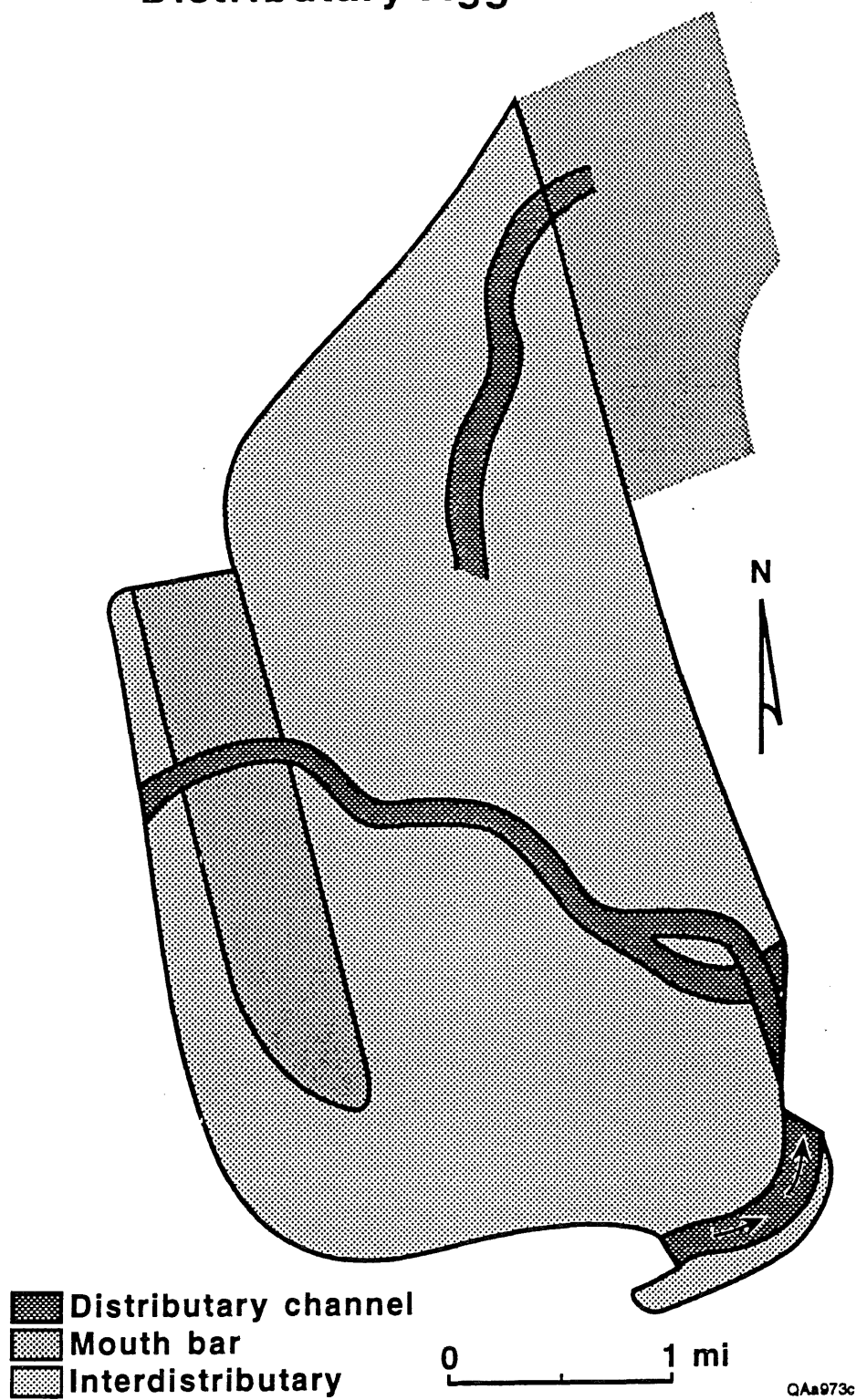


Figure 12. (b) Map of facies architecture in aggradational Ferron GS 2.

landward locations such as I-70, mouth-bar deposits are capped by small isolated barrier island sands that locally contain tidal channels. At seaward positions such as Dry Wash, rapid subsidence rates produced mouth-bar deposits that stack vertically and develop a thick sand-rich section. Laterally, mouth-bar sands thin and interfinger with finer grained, low-permeability distal delta-front, bar-flank, interdistributary-bay, and -marsh deposits, which will compartmentalize sidelapping mouth-bar deposits.

### Permeability Variation of Facies

By comparing stratal architecture with permeability values we can evaluate how depositional processes affect sandstone heterogeneity and determine what factors most significantly control permeability distributions. Three measures describe the permeability characteristics of different lithofacies groups: (1) permeability distribution type, interpreted from a cumulative frequency plot, (2) central tendency, estimated by the arithmetic mean, and (3) variance, estimated by the coefficient of variation.

Because different sedimentary processes operate in different depositional environments, we first explored permeability variation between the two volumetrically important facies in Ferron GS 2. Comparing cumulative permeability plots of distributary-channel and delta-front (distal mouth-bar) sandstones measured at the I-70 location, showed that distributary-channel sandstones have a significantly higher average permeability (166 vs. 74 md; fig. 13). Permeability in the distributary-channel facies varies considerably from less than 0.1 md to more than 1,000 md. The complex shape of the cumulative frequency plot indicates that samples from a single depositional facies represent a mixture of several permeability populations.

### Permeability of Distributary-Channel Sandstones

To resolve individual permeability populations, we divided the group of all distributary-channel permeability measurements into subsets according to geologic and lithologic

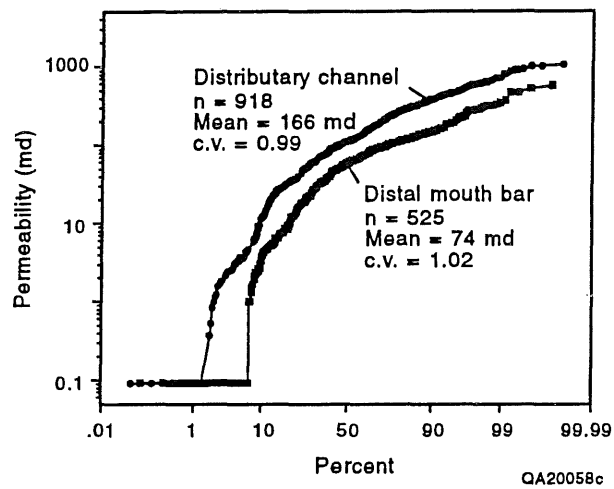


Figure 13. Plot of permeability versus cumulative percent for distributary-channel and delta-front facies.

characteristics. Much of the permeability variation in the distributary-channel samples is explained by lithofacies variation. A vertical profile (fig. 14) through distributary-channel and delta-front facies at I-70 shows the relationship between permeability, lithofacies, and depositional environment. These relationships provide a basis for separating distributary-channel samples into groups that represent different fluid-flow regimes during deposition: (1) ripple cross-stratified deposits, (2) horizontally stratified deposits, (3) trough cross-stratified deposits, (4) channel-lag deposits, and (5) fine-grained sediments and organic matter. Table 2 provides a description of lithologic characteristics, distribution, and permeability characteristics of each group.

Figure 15 shows log permeability versus cumulative percent relations for the five groups. Straight line segments on this plot indicate that ripple cross-stratified, trough cross-stratified, and horizontally stratified sandstones represent single, log-normally distributed permeability populations. Within each of these groups, permeability is mainly related to grain size. Permeability of lag deposits and fine-grained, organic-rich sediments are not log-normally distributed. These patterns probably reflect a large number of permeability determinations below the minipermeameter detection limit, as well as multiple populations within each group.

The range of permeability values displayed in figure 15 indicates that the five sedimentologically distinct groups form three permeability classes: (1) trough crossbedded and horizontally stratified sandstones (permeability of 10–1,000 md), (2) ripple stratified sandstones and fine-grained or organic-rich sediments (permeability of 0.1–10 md), and (3) lag deposits with intermediate permeability values (1–100 md).

The distribution of lithofacies and the permeability variation show a close association with the nature of the distributary-channel fill. Figures 16 and 17 compare bedform diversity and permeability distribution, respectively, for each macroform type. Cut-and-fill macroforms, located in the lower portion of the channel, are separated by erosional discontinuities and generally lack complete stratal successions. As a result, this facies displays a low bedform diversity characterized by trough cross-stratified sandstones and sand-rich lag deposits (fig. 16). In contrast, the higher preservation potential of the low-sinuosity macroforms results in greater bedform diversity

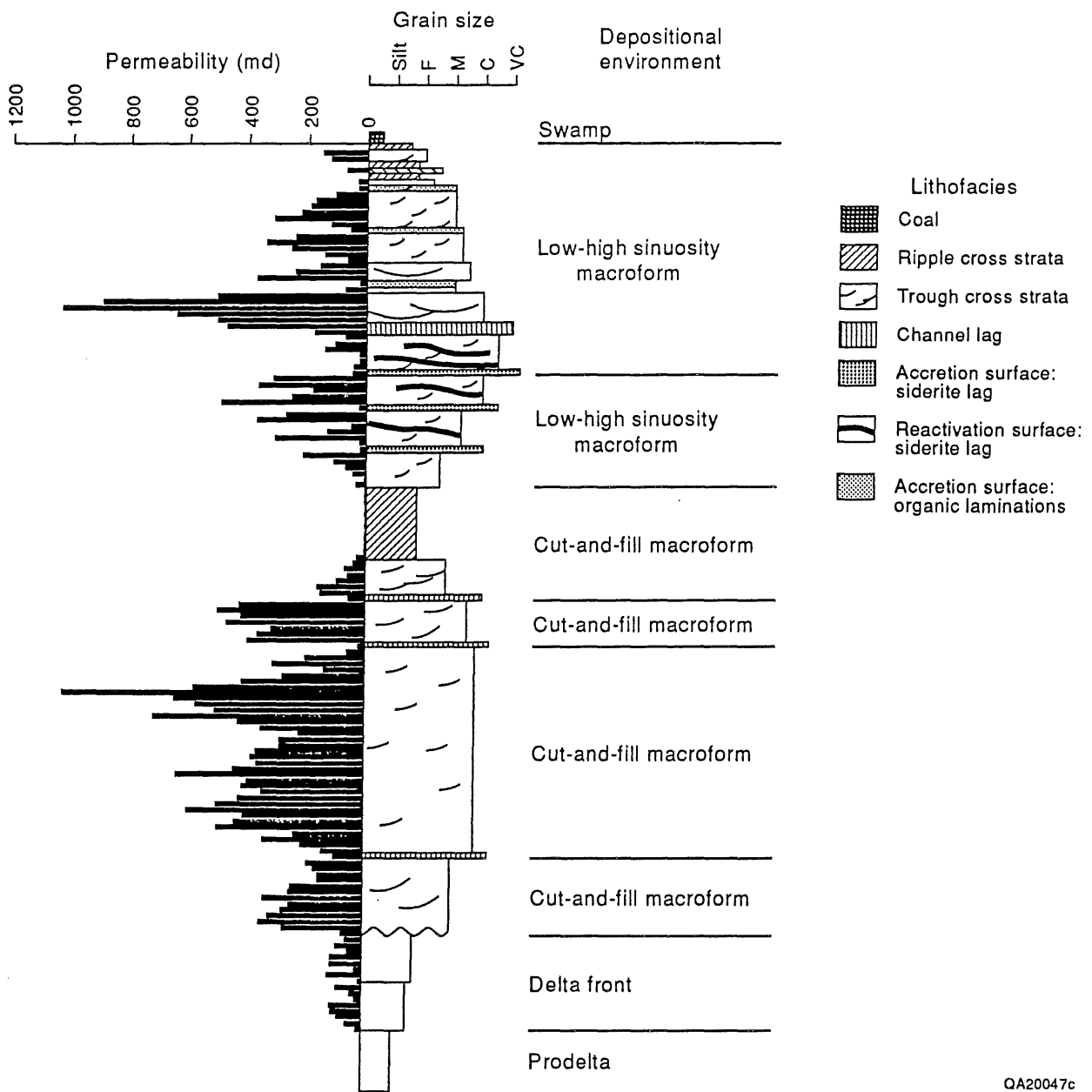


Figure 14. Vertical permeability profile through distributary channel.



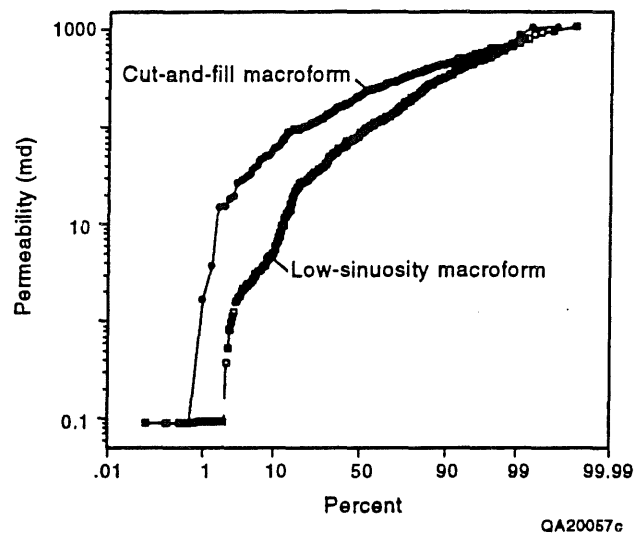


Figure 17. Plot of permeability versus cumulative percent for distributary-channel macroforms.



characterized by multiple bounding surfaces and a variety of sedimentary structures. These differences are reflected in a plot of log permeability versus cumulative percent for the two macroform types (fig. 17). The downward shift in the distribution curve from the cut-and-fill macroform to the low-sinuosity macroform reflects the fact that permeability variation increases with increasing bedform diversity.

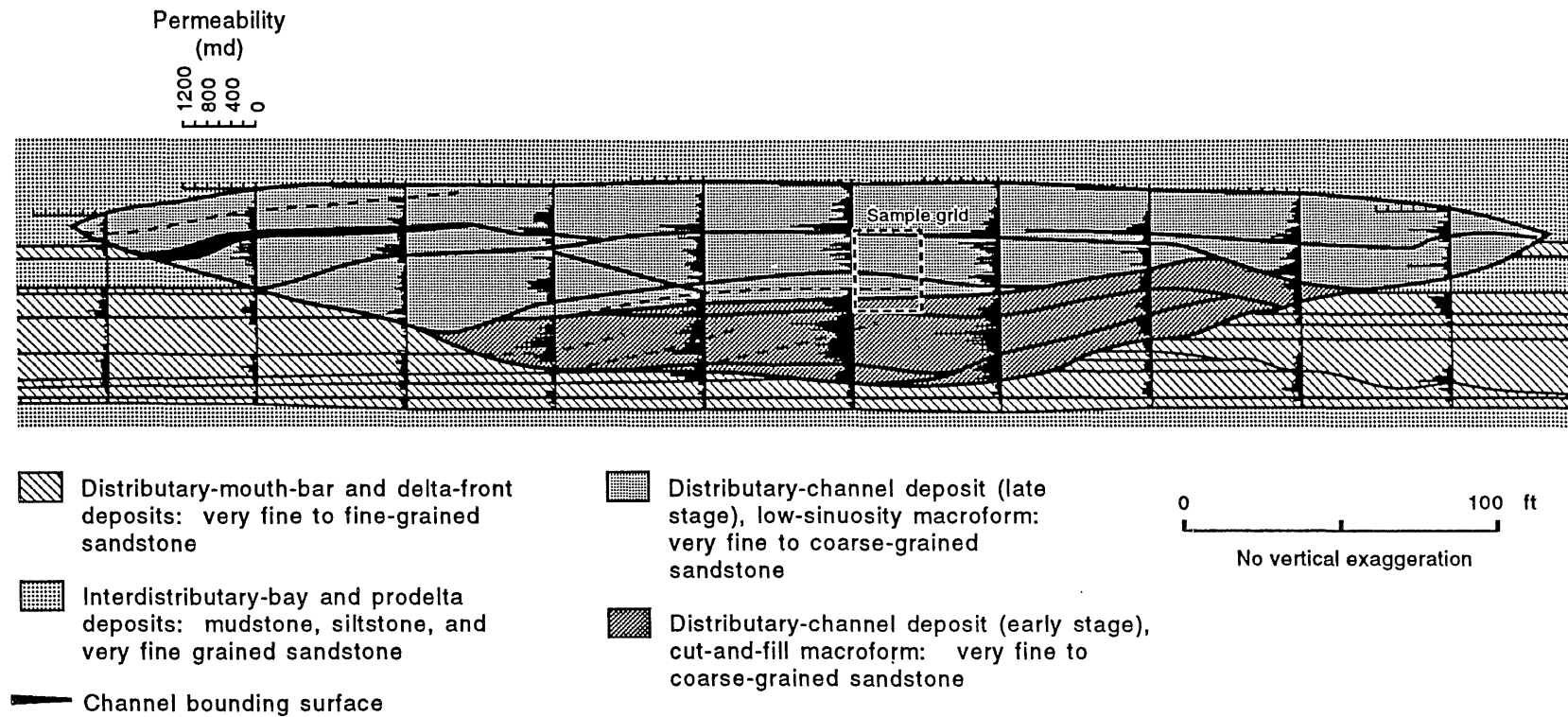
### Permeability Structure

To explore spatial variability in the distributary-channel sand body we measured permeability every 0.5 ft along a series of vertical transects spaced 50 ft apart. In addition, we constructed a 20- × 30-ft sample grid and detailed transects to examine permeability variation within a single macroform. We used both correlation of permeability profiles and construction of variograms to examine permeability relations.

#### *Permeability Correlation by Profile Comparison*

By visually comparing permeability profiles we can estimate how far along the outcrop's similar permeability profiles extend. The two criteria used to distinguish permeability trends from random fluctuations are: (1) a trend exists if permeability regularly increases or decreases along a transect as opposed to showing a single-point excursion and (2) a regular trend exists if an upward-increasing or -decreasing profile related to lithologic changes persists between transects.

Figure 18 shows the relationship of stratal architecture (bounding surfaces between and within macroforms) to permeability profiles for the GS 2 distributary-channel complex. Vertical permeability profiles show three distinct trends: (1) a cyclic pattern in the lower channel fill, (2) an erratic upward-increasing trend in the middle channel fill, and (3) an upward-decreasing trend in the upper channel fill. The high degree of similarity between adjacent profiles indicates that the observed permeability patterns are not random but extend laterally as much as several hundred feet.



QAa943(a)c

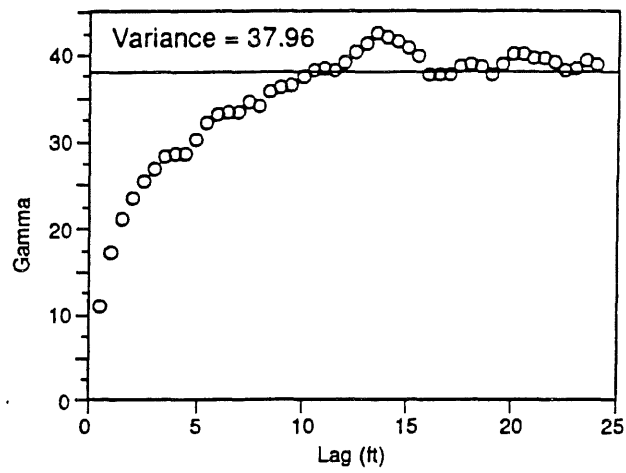
Figure 18. Facies architecture and permeability profiles of distributary-channel sandstones.

Comparison with the stratal architecture (fig. 18) demonstrates that bounding elements between macroforms define large-scale permeability trends. Cut-and-fill macroforms are characterized by a uniform permeability trend (3–12 ft thick) that extends laterally 100 to 250 ft. Low-sinuosity macroforms are characterized by an upward-increasing or -decreasing trend (10–20 ft thick) that extends laterally 200 to 350 ft. Overall, the permeability patterns in the distributary channel represent a composite of trends whose character and distribution reflect the highly amalgamated, multistoried nature of the channel fill. The classic upward-decreasing permeability trend most often modeled in reservoir simulations of channel sandstones is represented only by the final filling event in this channel complex.

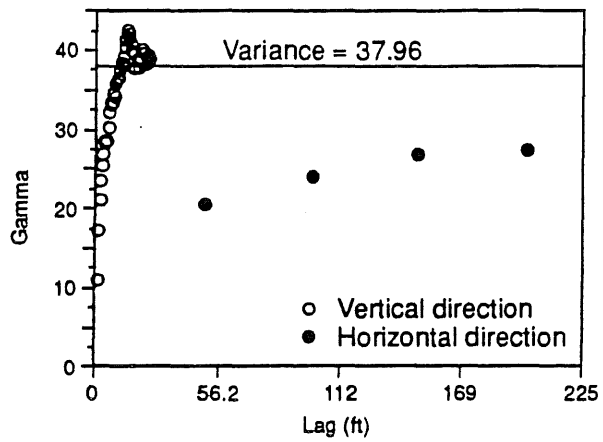
#### *Permeability Correlation by Semivariograms*

Semivariograms indicate spatial similarities between separate measurements. In studies of permeability structure, we can use semivariograms to determine ranges of permeability correlation and predictability. Figure 19a and b shows vertical and lateral semivariograms for the permeability data collected at 0.5-ft spacings along a series of vertical transects within the GS 2 distributary-channel complex. The results indicate that permeability measurements are related over a distance of 10 to 12 ft vertically and approximately 150 ft laterally. These dimensions correspond to the average vertical and lateral macroform dimensions (fig. 18).

Differences in the permeability structure between the cut-and-fill macroform and the low-sinuosity macroform type are reflected in the semivariogram function. Figure 20 displays the vertical variograms for each macroform type, normalized with regard to mean permeability, so that permeability variations can be directly compared. Permeability is correlated differently for each macroform type. Permeability structure in the cut-and-fill macroform reflects correlation over 2 to 4 ft that reflects the contrast between the trough crossbedded sandstone and lag deposits. Permeability structure within the low-sinuosity macroform reflects several types of correlation that



QA20051c



QA20050c

Figure 19. (a) Vertical variogram for distributary-channel facies. (b) Horizontal and vertical variograms for distributary-channel facies.

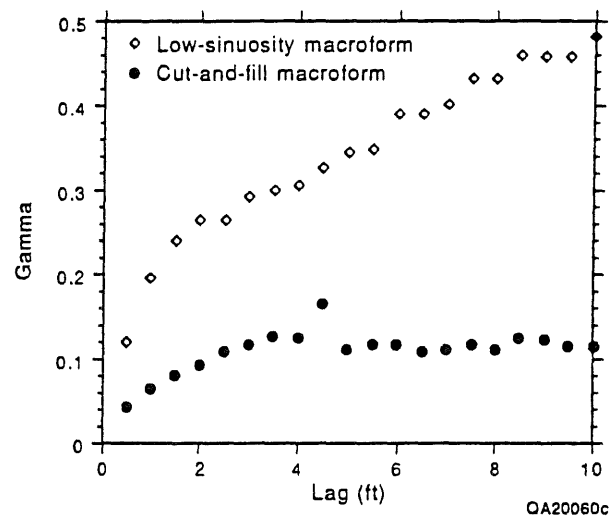


Figure 20. Vertical variograms for low-sinuosity and cut-and-fill distributary channel types.

for distances less than 2 ft are related to bounding surfaces and for distances greater than 2 ft are related to upward-increasing or -decreasing permeability trends.

### *Scale Dependence of Permeability*

To investigate fine-scale permeability structure we constructed a 20 × 30 ft grid with measurements at 1-ft spacing and an embedded series of 4-ft vertical transects with 0.25 ft between measurements. The grid contains both cut-and-fill and low-sinuosity macroforms. In the lower portion of the grid a cut-and-fill macroform with an erosive base, represented by a thin lag deposit, is overlaid by amalgamated trough crossbedded strata and is capped by massive to ripple-laminated strata. Erosively overlying this unit is a sequence of trough crossbedded strata with well-developed internal accretionary sets and reactivation surfaces. Grain size increases upward from fine to coarse sand. This sequence represents either downstream or lateral accretion of a low-sinuosity macroform. Near the top of the grid is part of a third macroform that eroded into the underlying sands and represents the final fill event of the distributary-channel complex.

Figure 21 shows sample grid, primary lithologic attributes and their spatial distribution, and four typical permeability profiles. Three vertical, scale-dependent permeability trends exist. At the largest (first order) scale, permeability increases stepwise upward from base to top of the macroform. Within the low-sinuosity macroform are distinct permeability zones 3 to 5 ft thick (second order). Some of these zones contain small-scale (third order) permeability trends, 0.5 to 1.5 ft thick. Variations in grain size, sorting, and the presence of lithologic discontinuities, generally control these permeability variations. Comparison of permeability profiles indicates a high degree of lateral correlation with distinct permeability zones paralleling the low-angle inclined accretion surfaces (third-order zones of heterogeneity). On the basis of the correlation of permeability variation with stratal architecture, we interpret these zones to be 50 to 75 ft long. Smaller scale (fourth order) permeability trends that also parallel accretionary surfaces exist within these units. These zones are

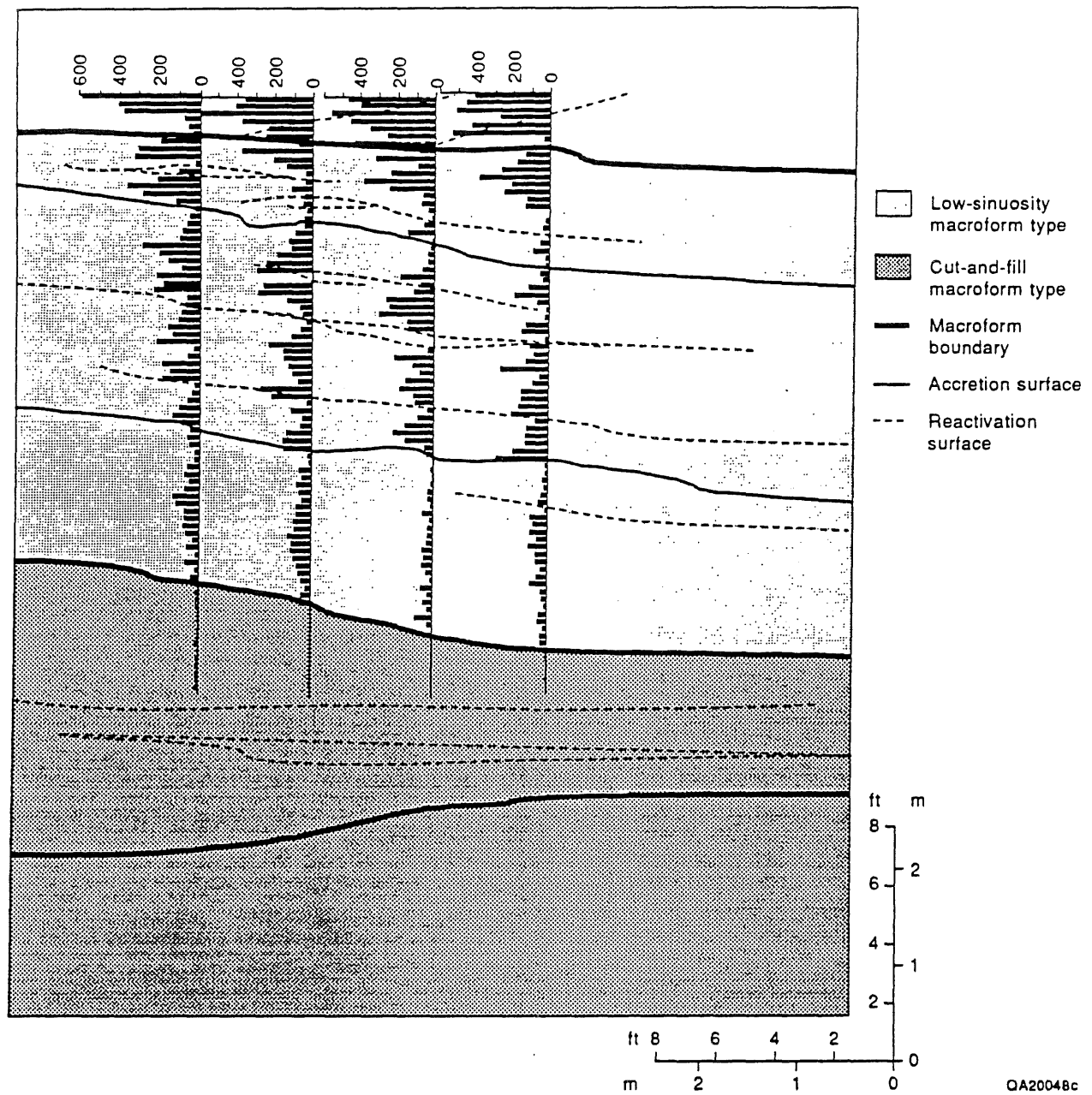


Figure 21. Architecture and permeability profiles for detailed grid from distributary-channel facies.

related to reactivation surfaces within accretionary units. Individual zones have lengths of 10 to 20 ft.

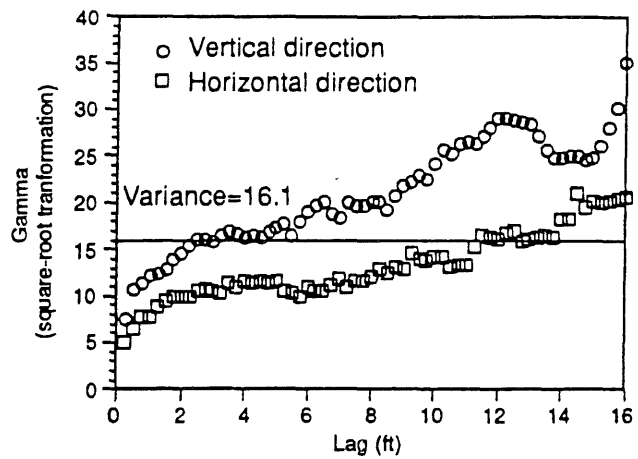
Figure 22 shows the vertical and horizontal semivariograms calculated for the sample grid. The vertical correlation range is 2 to 4 ft, and the horizontal correlation range is about 14 ft. Changes in slope of the semivariogram function reflect three scale-dependent types of vertical permeability pattern. From smallest to largest scale, these are (1) fifth-order heterogeneity related to reactivation surfaces (2 ft), (2) fourth-order heterogeneity related to accretionary sets (6 ft), and (3) third-order heterogeneity related to macroform type (12 ft).

### Distribution of Baffles

We operationally define a baffle as a discontinuous interval of low-permeability rock that would probably act as an obstacle to flow under reservoir conditions. Such intervals need not be continuous to severely affect directional permeabilities in a reservoir (Haldorsen and Lake, 1984). Because the distributions and dimensions of baffles are impossible to describe solely from core or well logs, it is important to quantify them on outcrop. Baffles within genetic units probably have characteristic shapes and distributions that are related to depositional processes. Understanding these processes will provide a basis for predicting baffle properties and distributions in sandstone reservoirs.

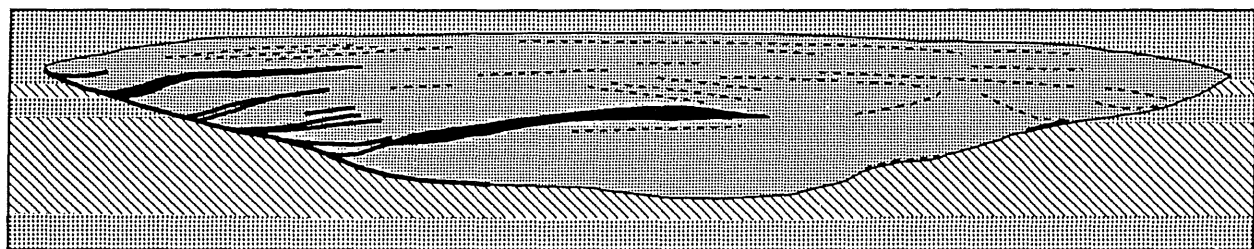
To characterize the geometry of baffles we mapped the distribution of low-permeability intervals on photomosaic panels. Lithologically, the low-permeability units are either thin shale layers or sandstone intervals tightly cemented by hematite and clay. Shales form thin discontinuous layers that drape lateral accretion sets and channel margins. Clay- and hematite-cemented sandstones form thin discontinuous layers along erosional surfaces such as reactivation surfaces, accretion surfaces, and channel margins (fig. 23). Individual baffles have limited lateral extent; none extend across the entire channel facies, and they rarely correlate with the adjacent transect. However, along horizons of greater lateral extent, such as channel margins, baffles regularly





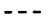


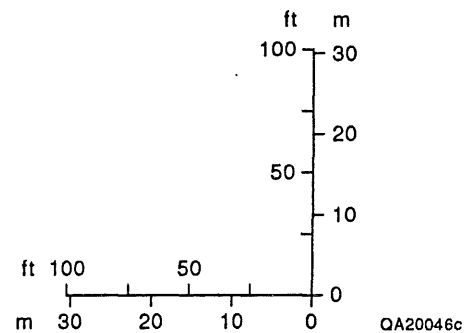


QA20053c

Figure 22. Horizontal and vertical permeability semivariograms determined from the detailed grid in the distributary-channel complex.



-  Distributary-channel facies: very fine to very coarse grained sandstone
  -  Delta-front facies: very fine to fine-grained sandstone
  -  Interdistributary bay and prodelta: very fine grained sandstone, siltstone, and mudstone
  -  Shale layer
  -  Baffle
- } (lithofacies with permeability less than 1.0 md)



QA20046c

Figure 23. Distribution of permeability baffles in distributary-channel complex.

reappear. Figure 24 shows a cumulative frequency curve of baffle lengths; 50 percent are about 50 ft long, and few extend more than 100 ft. The spatial distribution of each baffle type shows a high dependence on macroform type; therefore, the existence of similar baffles in analogous reservoirs is predictable.

### Permeability of Delta-Front Sandstones

Delta-front permeability measurements were divided into subset populations according to geologic and lithologic characteristics (table 3). Permeability in the delta-front facies averages 170 md and displays a high degree of variability, ranging from less than 0.1 md to almost 1,000 md. A plot of log permeability versus cumulative probability (fig. 25) for the delta-front facies demonstrates that the data cannot be characterized as either normally or log-normally distributed. Instead, the data fit a distribution type that is multimodal, as indicated by the changes in slope at approximately 10 and 300 md. Similar to the distributary-channel facies, permeability at the facies scale is not represented by a single population but instead by a mixture of several populations.

A plot of log permeability versus cumulative percent shows a close relationship between permeability and original bedding type (fig. 26), indicating that much of the permeability variation is explained by lithofacies variation. Permeability values indicate that lithofacies groups form four permeability classes: (1) trough and low-angle inclined cross strata with average permeabilities between 100 and 1,000 md, (2) planar parallel strata, bioturbated, contorted, and massive bedded lithofacies groups with average permeabilities between 10 and 100 md, (3) hummocky and ripple cross strata with average permeabilities between 1 and 10 md, and (4) mudstone, siltstone, and wavy laminated lithofacies with average permeabilities between .01 to 1 md. Straight-line segments on the cumulative probability plot indicate that lithofacies groups represent single, log-normally distributed permeability populations.

Permeability variation within delta-front sediments is closely related to textural and compositional characteristics. For example, a comparison by stratal types shows a predictable

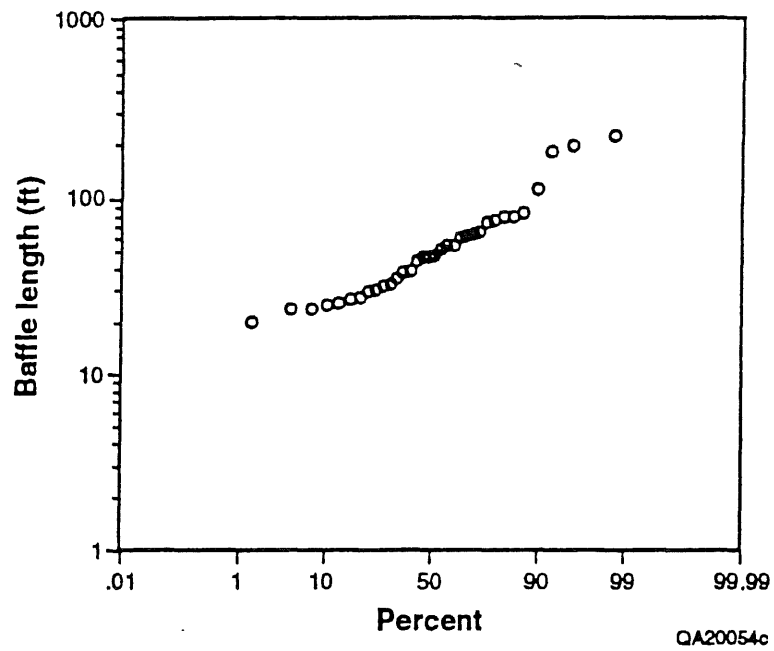


Figure 24. Plot of baffle length versus cumulative percent for low-permeability strata in the distributary-channel complex.

Table 3. Permeability characteristics of facies and lithofacies.

Facies	Number	Mean (md)	Coefficient of Variation
Prodelta	19	0.3	1.2
Interdistributary bay	78	2.9	1.03
Crevasse splay	10	6	1.2
Bar flank	256	27	1.42
Distal delta front	160	54	0.56
Slump	77	59	1.14
Proximal mouth bar	142	255	0.56
Wave-modified mouth bar	271	419	0.35
<b>Lithofacies</b>			
Wavy bedded	29	0.9	1.3
Hummocky	63	8.3	0.56
Ripple	127	17	0.89
Contorted	46	57	0.99
Plane parallel	126	66	0.78
Massive	38	76	0.89
Trough	280	336	0.37
Low angle	112	456	0.27

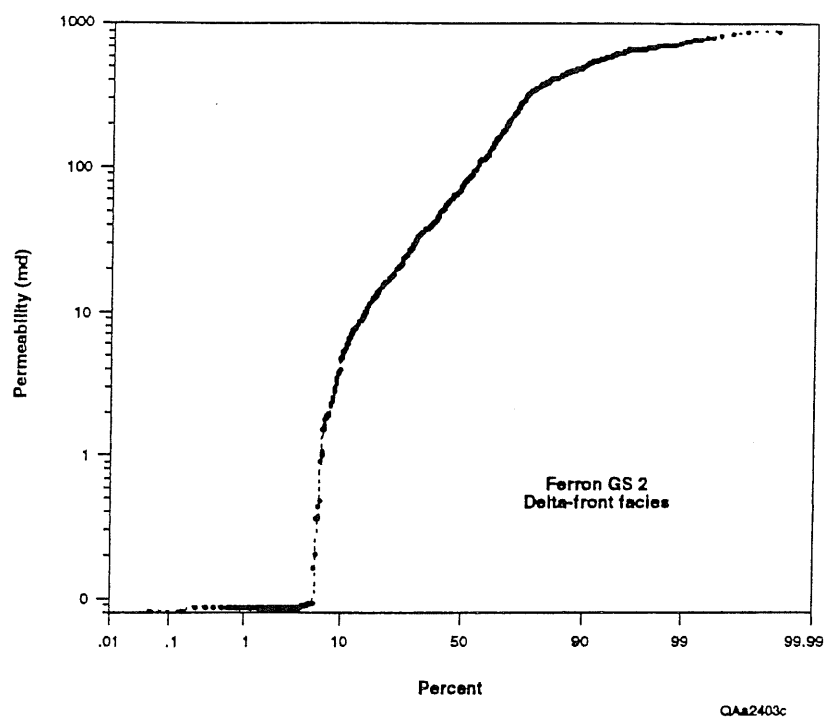


Figure 25. Plot of permeability versus cumulative percent for delta-front sandstones.

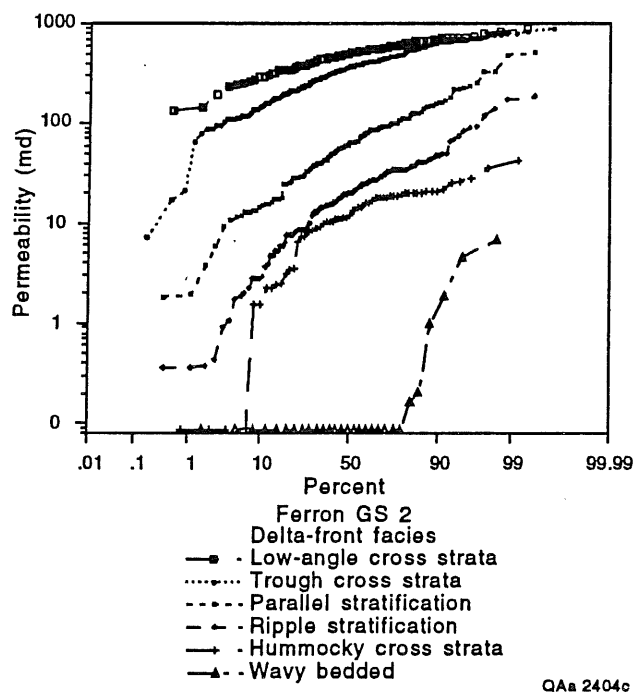


Figure 26. Plot of permeability versus cumulative percent for delta-front lithofacies.

increase in permeability with increasing grain size. Very fine to fine-grained ripple-stratified sandstones display the lowest permeabilities, fine-medium-grained, low-angle stratification type display intermediate permeabilities, and medium-fine to coarse-grained trough cross-stratified sandstones display the highest permeabilities. Permeability also increases with increased sorting with medium-grained trough cross strata from the wave reworked mouth-bar facies, displaying approximately twice the permeability as the medium-grained trough cross strata from the fluvially dominated mouth-bar facies.

Lithofacies form common associations termed facies. Figures 27 and 28 compare bedform diversities and permeability distributions, respectively, for each facies type. Wave-modified and proximal mouth-bar facies contain a high percentage of high-permeability lithofacies groups and thus would be good reservoir rocks. Slump deposits, crevasse splay and distal delta-front deposits form intermediate to poor-quality reservoir facies containing a high percentage of massive to contorted and bioturbated strata, respectively. Bar-flank, interdistributary-bay, and prodelta deposits are fine-grained, low-permeability strata that constitute nonreservoir quality rocks and potential barriers to gas flow.

#### Permeability Patterns and Reservoir Connectedness

Figure 29 shows the relationship of facies architecture to permeability profiles for the GS 2 delta-front deposits. Upward-increasing trends are well developed where mouth-bar facies prograde across finer grained bar-flank and distal delta-front deposits and are poorly developed where interdistributary-bay deposits overlie distal delta-front deposits. Laterally, the central portions of the mouth-bar deposits display the highest permeability and the margins the lowest. Mouth-bar sands interfinger with bar-flank deposits and thin, high-permeability zones may extend several hundred to several thousand feet from the proximal portion of the deposit. In general, zones of high permeability are best developed in the upper portion of the sequences associated with wave-modified and fluvially dominated mouth-bar sands; however, zones of high permeability also occur

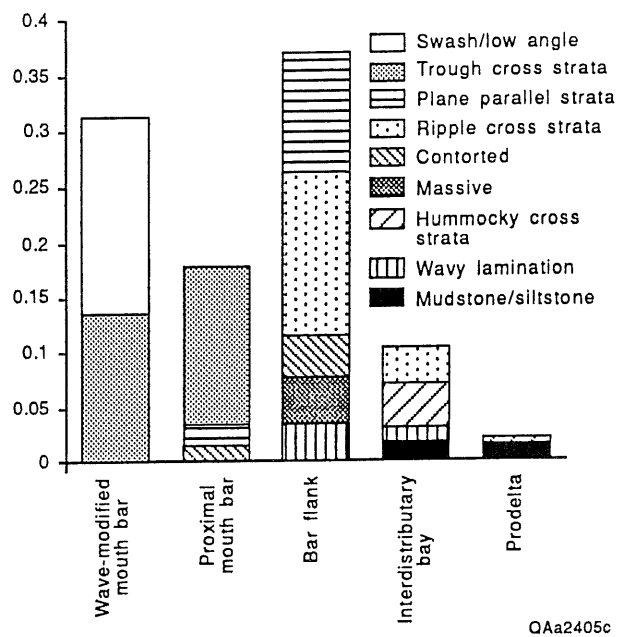


Figure 27. Bedform diversity within delta-front facies.

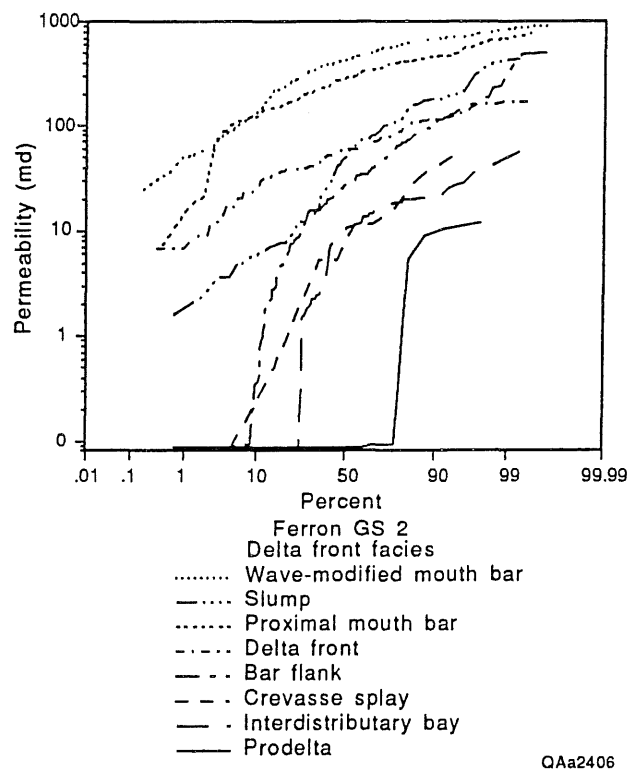
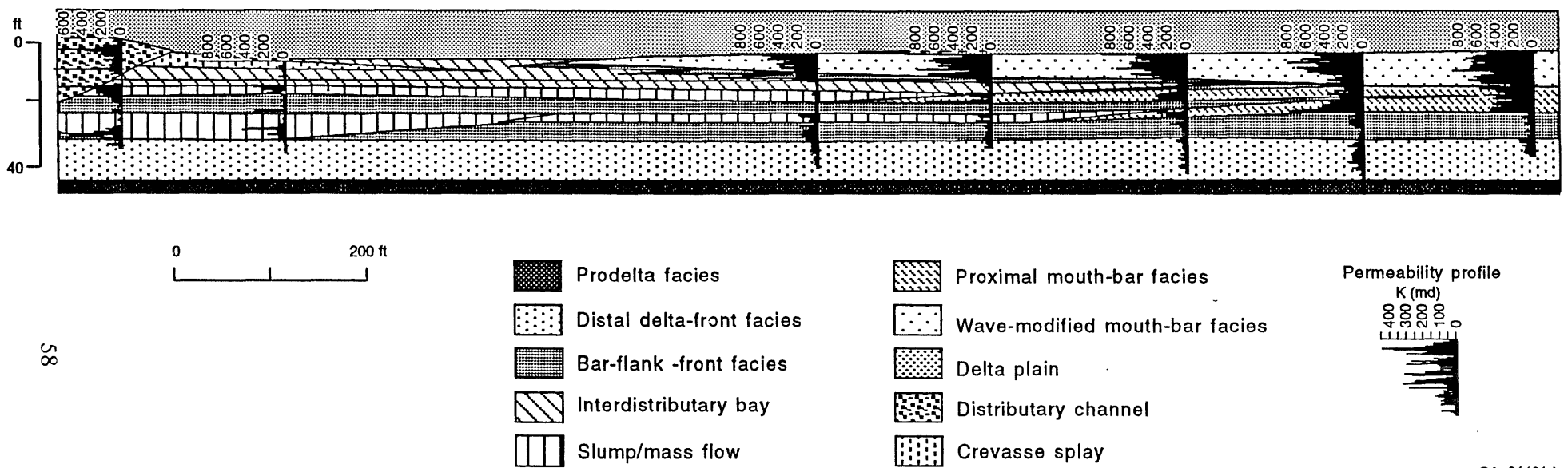


Figure 28. Plot of permeability versus cumulative percent for delta-front facies.





QAa2410(a)c

Figure 29. Facies architecture and permeability profiles of delta-front facies.

in the lower portion associated with slump and mass flow deposits that formed along the base of an advancing mouth bar.

The potential for large-scale (facies-scale) compartmentalization is significant. Prodelta and marsh-swamp deposits bound the base and top of GS 2, effectively preventing communication with underlying and overlying sequences. Within GS 2 reservoir quality sand bodies are extremely compartmentalized. Wave-modified mouth-bar sands are isolated from one another and from underlying sands by interdistributary-bay and -marsh deposits. Fluvially dominated mouth-bar deposits are isolated by heterolithic bar-flank and interdistributary-bay deposits from underlying and laterally adjacent sands. Slump and mass flow deposits are isolated from one another and from adjacent mouth-bar deposits by prodelta and bar-flank sands. Although sand bodies display a high degree of external compartmentalization, internally they are relatively homogeneous. With the exception of the bar-flank facies, few discontinuities are present.

## PETROGRAPHY AND DIAGENETIC OVERPRINT

### Methods

Sandstone reservoirs have a long and complex history from initial sediment deposition through burial, compaction, cementation, porosity generation and reduction, and gas emplacement. Clearly, we cannot expect to understand and predict the distribution of reservoir architectural elements solely by studying depositional processes.

We conducted petrologic investigations in conjunction with outcrop studies to determine what mineralogic, textural, and diagenetic properties characterize flow units, baffles, and barriers, and to relate these properties to diagenetic history as well as to depositional processes. Major objectives of this work are to (1) establish the initial mineralogic composition of Ferron sandstones from various facies and environments so that we can evaluate differences between the outcrop analog and various sandstone gas reservoirs, (2) quantify changes caused by burial and diagenesis

and the associated effects on porosity, pore structure, and permeability, and (3) establish predictive relations between depositional systems, lithofacies, diagenetic effects, porosity, and air permeability.

The burial and thermal history of the Ferron Sandstone is discussed in our companion report (Fisher and others, 1993) and is only briefly summarized here. Initial subsidence was rapid and burial depths of approximately 10,000 to 14,000 ft were attained. Maximum sustained burial temperatures, estimated from coal composition and vitrinite reflectance data, were 65° to 80° C. These relatively cool temperatures agree with the observations that neither feldspars in Ferron sandstones nor illite/smectite in Mancos shale has undergone extensive alteration from detrital compositions.

We selected samples on the basis of mapped facies relations and field-measured permeabilities; our intent was to collect sandstones that represent typical, volumetrically important sand bodies (presumed to act as flow units under reservoir conditions), sandstones near the margins of the major macroforms (commonly permeability anomalies), and bounding elements (presumed to act as baffles or barriers under reservoir conditions). Most samples were 1-inch-diameter cores, 3 to 6 inches long, that were drilled from outcrop with a portable core plugger. We also collected large sandstone blocks of presumed flow units, baffles, and barriers for combined petrophysical and petrographic analysis.

We visually examined each sample, measured permeability using the field minipermeameter, and prepared a thin section for petrographic examination. On the basis of preliminary microscopic examination, we selected a subset of samples and quantified framework grain mineralogy, cement mineralogy, intergranular volume, and porosity using standard petrographic microscope techniques. Clay mineralogy for a representative suite of samples was determined by standard X-ray diffraction techniques. Scanning electron microscopy and other chemical or isotopic analyses were performed on a select group of samples to help resolve the history of diagenetic processes.

## Results

### Framework Grain Composition

Quartz, feldspar, and rock fragments are the basic detrital components of Ferron sandstones. Common quartz with straight to slightly undulose extinction is by far the most abundant quartz type present. Contacts between quartz grains are typically concavo-convex to sutured, indicating that pressure solution has occurred. Potassium feldspar is more abundant than plagioclase, particularly in the coarser-grained sandstones. Potassium feldspar is usually fresh although minor amounts of partially leached potassium feldspar exist. Plagioclase grains may be fresh, highly sericitized or vacuolized, or partly to totally leached. Leached plagioclase and potassium feldspar provide microporosity that is recorded in the point-count data only if it amounts to more than 50 percent of the original feldspar grain volume.

The lithic component of Ferron sandstones is mostly chert and low- to medium-grade metamorphic rock fragments. Both chert and metamorphic rock fragments occur as fresh to highly leached grains. Significantly, the types of rock fragments present in the Ferron are relatively ductile grains that deform around more rigid quartz and feldspar during burial and compaction, thus reducing porosity and permeability.

Ferron GS 2 distributary-channel sandstones are quartz-rich arkoses with minor amounts of lithic arkose and subarkose sandstones (fig. 30). Delta-front and mouth-bar sandstones overlap the compositional field of distributary-channel sandstones but are generally more quartz rich (fig. 30). Most delta-front and mouth-bar sandstones are subarkoses, although some arkoses and quartzarenites are present.

### Intergranular Material

Authigenic cements, porosity, and pseudomatrix fill the volume between detrital grains. Authigenic phases are predominantly either quartz or kaolinite; only traces of carbonate occur in

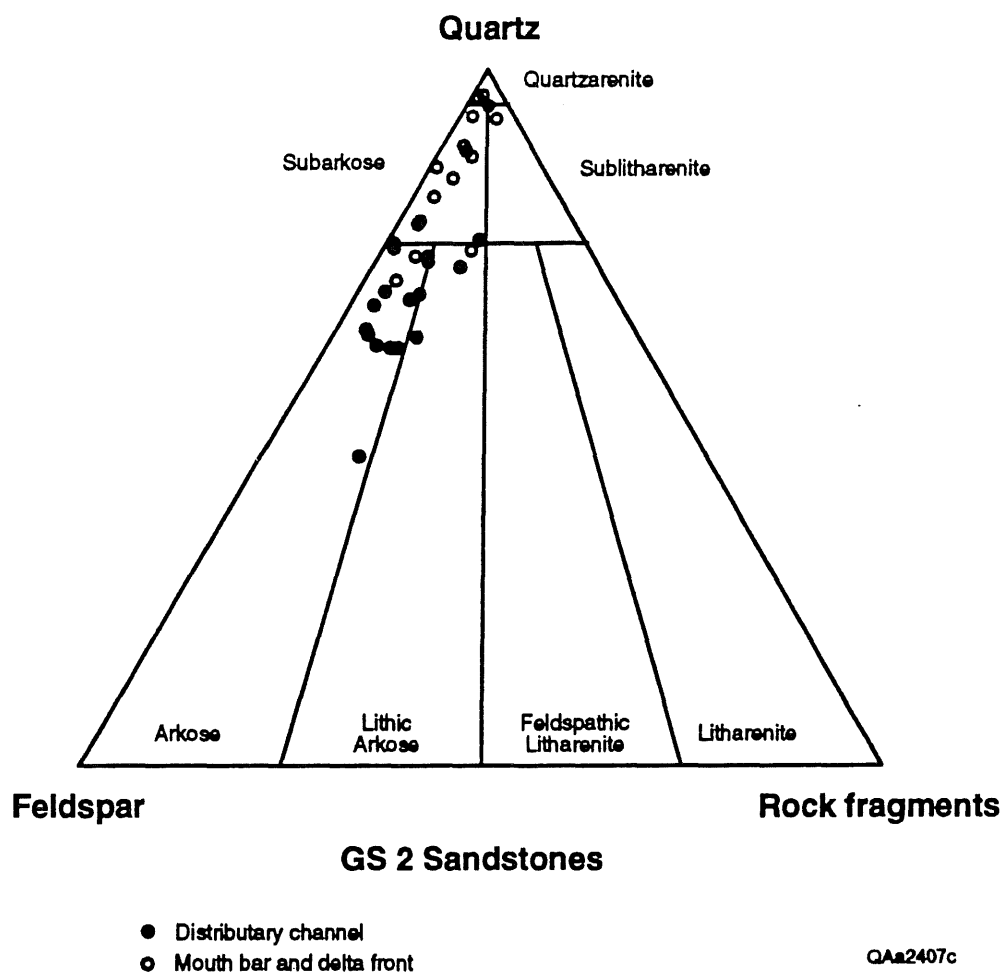


Figure 30. Framework grain composition of sandstones from Ferron GS 2 (classification of Folk, 1974).

GS 2 sandstones. Kaolinite occurs mainly as pore-filling cement; less commonly it has a texture that reflects grain replacement. Quartz cement forms overgrowths on detrital quartz grains. Concavo-convex and sutured quartz-quartz grain contacts record the effects of pressure solution and silica mobilization during burial compaction.

Ferron GS 2 sandstones contain both macroporosity and microporosity. Macroporosity is present as intergranular void space and as voids left by complete grain dissolution. Microporosity exists within partly leached grains (mostly plagioclase and chert fragments) and between crystallites in patches of authigenic kaolinite. Much of the macroporosity would be classified as secondary porosity according to the criteria of Schmidt and MacDonald (1979). Undoubtedly, some of the primary intergranular porosity that existed before the strata were uplifted during late Miocene to Holocene time (approximately 10 to 15 mya) has been enhanced by dissolution at the outcrop.

Pseudomatrix consists of locally derived clay rip-up clasts and mud and coal chips. After burial compaction, clay and mud clasts are indistinguishable from clay laminae and clay or mud introduced by bioturbation. Because clay clasts could not survive transport over any significant distance, and because they now so closely resemble bioturbated laminae, they are classified as intergranular material rather than detrital grains. Like rock fragments, pseudomatrix readily deforms during burial compaction and severely reduces porosity and permeability by filling intergranular space. Pseudomatrix typically has weathered to a combination of Fe-Mn-oxide, Fe-Mn-hydroxide, and pyrite during exposure on the outcrop. Petrographic relations show that no appreciable volume change accompanied this conversion, thus it did not affect rock texture.

In distributary-channel, delta-front, and mouth-bar sandstones of Ferron GS 2, quartz and kaolinite are the predominant authigenic phases. Carbonate cement and authigenic iron sulfides or iron oxyhydroxides are present but rare. Total cement volume in Ferron GS 2 sandstones is low, seldom exceeding 4 to 5 percent. Because of the low burial temperatures, Ferron sandstones have had only a mild diagenetic overprint.

Although compositionally different from the equivalent facies in Ferron GS 5, Ferron GS 2 sandstones show some of the same relations we observed in the landward-stepping GS 5. In GS 5 we

found that distributary-channel sandstones are more permeable than delta-front sandstones and that the increase in mean permeability of distributary-channel sandstones from landward to seaward extent of the facies tract is accompanied by a mineralogic shift to compositions with lower rock-fragment content. We attributed the more quartz-rich compositions of delta-front and transgressive sandstones to physical reworking in the depositional environment. A seaward increase in reworking effectiveness also probably reduced the amount of ductile rock fragments that reduce porosity during compaction. We were able to sample Ferron GS 2 at only one location, near the center of the facies tract. Therefore we cannot make landward-to-seaward compositional comparisons as we did for GS 5. However, in both GS 2 and GS 5, the sandstones which were most reworked in the depositional environment are the most quartz rich. In GS 5, we found that transgressive and delta-front sandstones contained more detrital quartz than distributary-channel sandstones. In GS 2, mouth-bar and delta-front sandstones were more thoroughly reworked prior to final deposition than distributary-channel sandstones. The higher quartz-to-feldspar ratio of mouth-bar and delta-front sandstones reflects this difference.

Comparison of GS 2 and GS 5 sandstone compositions and permeability relations, therefore, reveals some common principles. Although the actual compositions of equivalent facies differ between the two genetic sequences, mineralogic relations between facies within a sequence are similar. Therefore, unless obliterated by diagenetic processes, sandstone mineralogy and mineralogy-permeability relations can be anticipated from a knowledge of depositional processes, sequence stratigraphic setting, and position in the facies tract.

#### IMPLICATIONS FOR INFILL DRILLING

Targeted infill drilling in known natural gas fields can be an effective and cost-efficient way to increase recovery of an important energy resource. One of the major goals of our Ferron Sandstone outcrop characterization study is to provide guidelines for maximizing the yield of additional wells in areas of known gas production.

To investigate how conventional drilling would contact Ferron GS 2 reservoir-analog sandstones we first combined the maps of the regressive (fig. 12a) and aggradational (fig. 12b) portions of GS 2 (fig. 31). Assuming burial and gas migration into the Ferron reservoir analog and using this hypothetical reservoir to evaluate the degree of contact in a conventional infill drilling program, we can analyze the effectiveness of drilling wells at various spacings. Because most of the sand in the seaward-stepping genetic sequence is stored in the mouth-bar system, this facies constitutes a principal reservoir target despite the somewhat lower mean permeability relative to distributary-channel sandstones (74 md for mouth-bar deposits vs. 166 md for distributary-channel deposits).

Drilling at 640-acre spacing (fig. 32) requires 18 wells, of which 6 miss the distributary channel-mouth-bar complex and hit prodelta nonreservoir facies. At this spacing 41 percent of the reservoir area is contacted. Fifteen additional wells are needed to achieve 320-acre spacing (fig. 33). Of the 15 new wells, 2 are dry holes and 3 are marginal. After drilling at 320-acre spacing, 91 percent of the reservoir area is contacted.

This exercise indicates that seaward-stepping, fluvially dominated deltaic sandstones are relatively simple targets because the mouth-bar sandstone complex is areally extensive and has relatively good permeability. As in the landward-stepping Ferron GS 5, distributary-channel sandstones have the highest mean permeability. However, unlike GS 5 where distributary-channel deposits were laterally widespread, in GS 2 the distributary-channel sandstones are linear features that account for a small percent of the total reservoir facies. The seaward-stepping system is also elongated (~40 mi from proximal to distal end), unlike the landward-stepping, wave-modified Ferron GS 5. Of course, other factors besides mean permeability and areal extent affect reservoir performance. Chief among these is the degree of internal heterogeneity and the effectiveness of internal baffles and barriers. These factors can only be fully evaluated through flow modeling of three-dimensional reservoir representation. However, in the absence of flow modeling results, simple exercises such as those presented here provide guidelines for infill drilling decisions.



## Ferron GS 2 Composite Facies Architecture

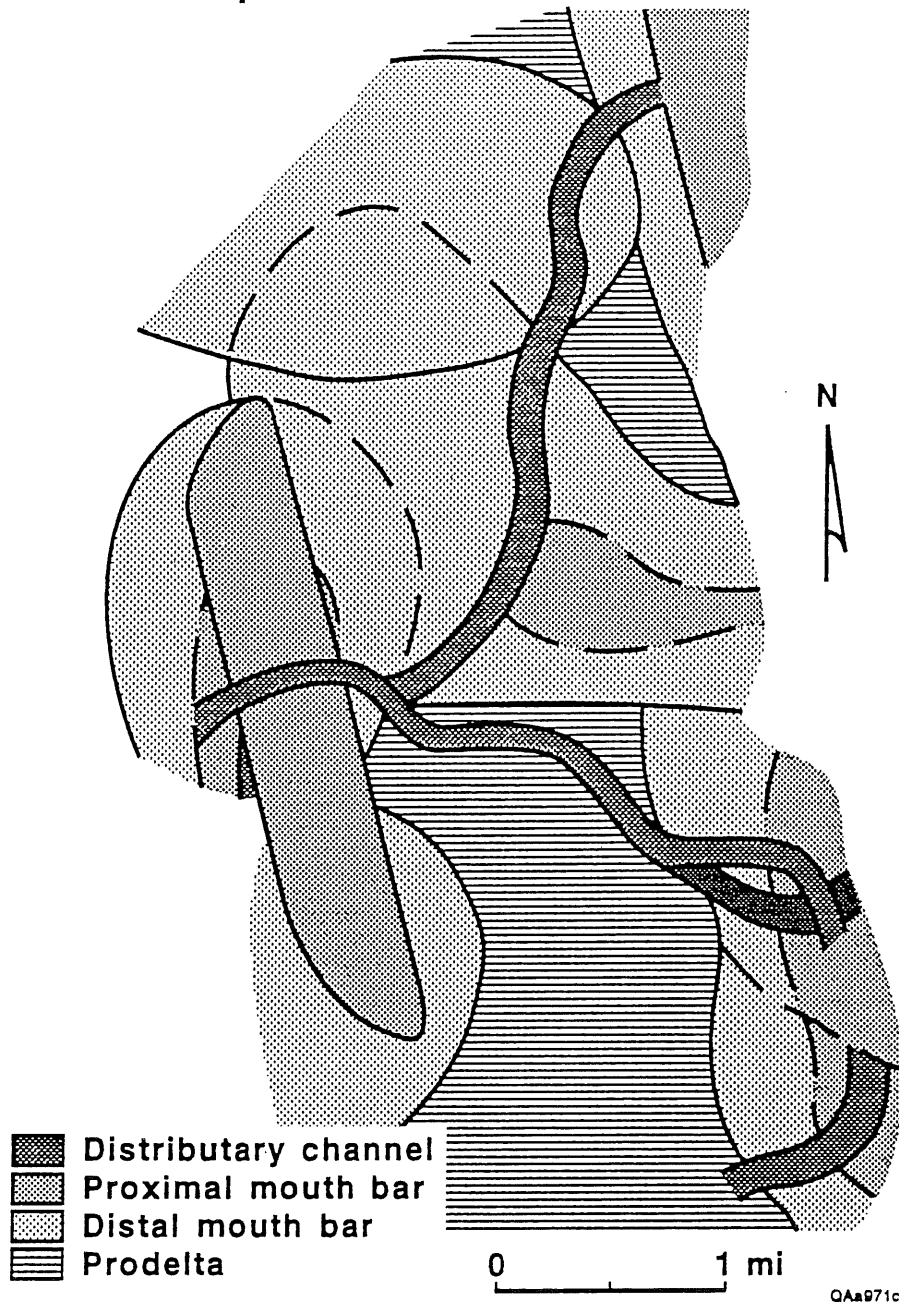


Figure 31. Composite field-scale facies architecture of regressive and aggradational distributary-channel and mouth-bar sandstones.

**Wells drilled**      18  
**Dry holes**         6  
**Area contacted** 41%

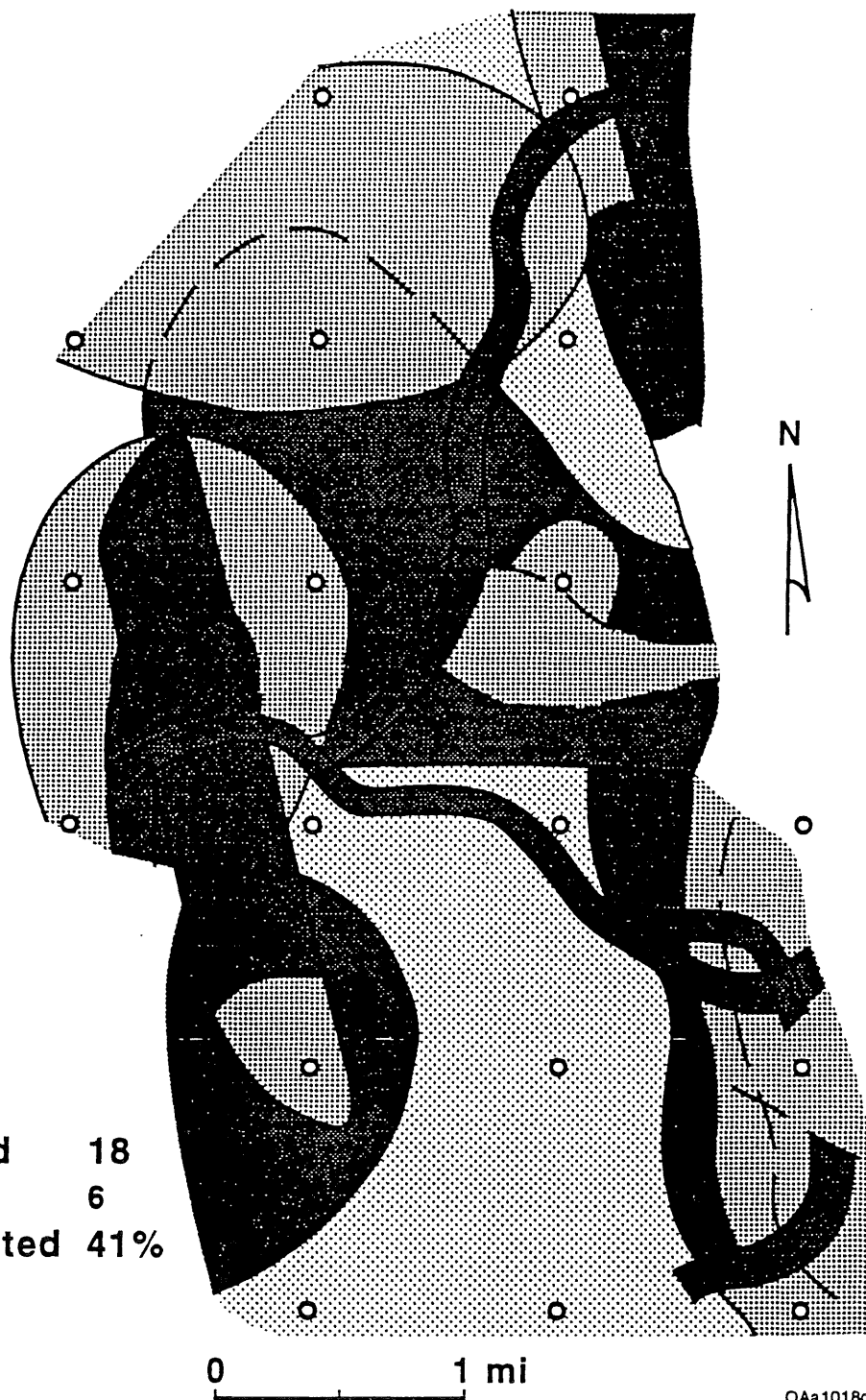


Figure 32. Composite field-scale facies architecture of Ferron GS 2 distributary-channel and mouth-bar sandstones showing effects of drilling at 640-acre spacing.

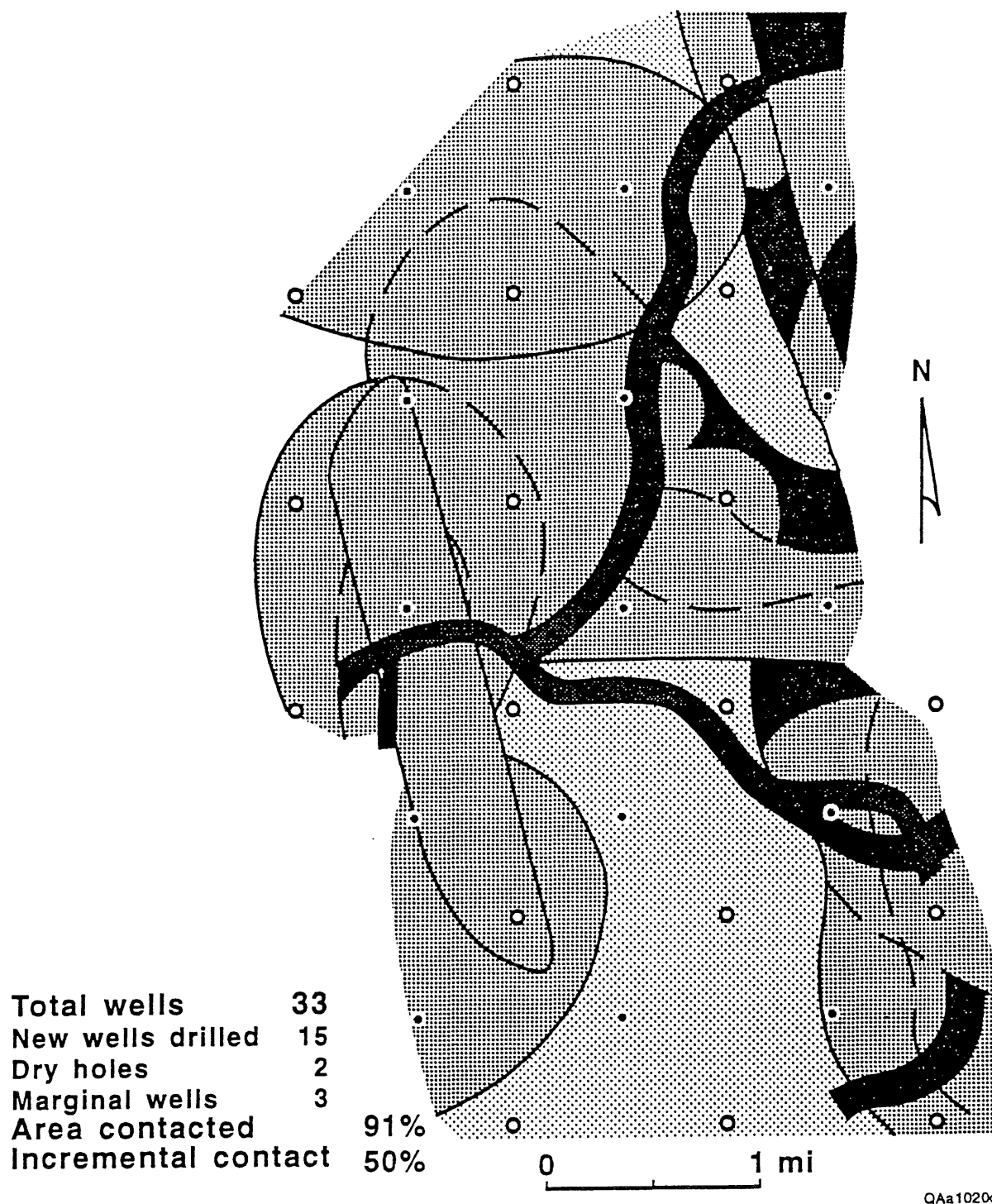


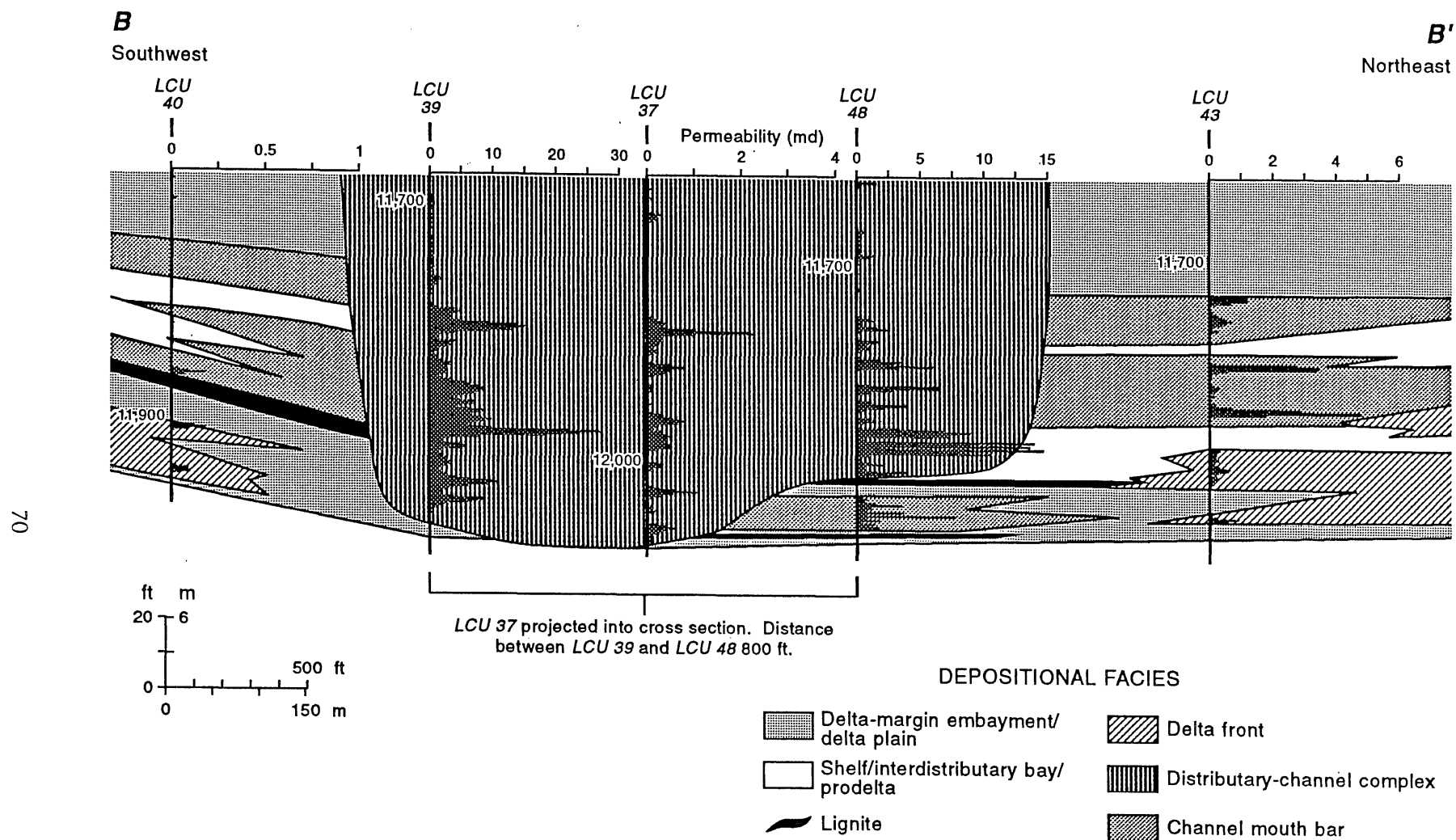
Figure 33. Composite field-scale facies architecture of Ferron GS 2 distributary-channel and mouth-bar sandstones showing effects of drilling at 320-acre spacing.

## FERRON OUTCROP—LAKE CREEK FIELD COMPARISON

An independent study of reservoir behavior in the Lake Creek field, Wilcox Group, Texas Gulf Coast, provides us a way to test the conclusions reached through outcrop characterizations of the Ferron Sandstone. The Lake Creek field study was conducted at the Bureau of Economic Geology and funded by the Gas Research Institute's Secondary Natural Gas Recovery Program. Preliminary results are summarized by Grigsby and others (1992).

The primary objective of the Lake Creek field study was to evaluate the potential for secondary gas recovery in deltaic reservoirs of the lower Wilcox Group, Tertiary, Texas Gulf Coast. Therefore this reservoir represents one of the types of reservoirs that we wish to better understand through the Ferron outcrop study. Detailed stratigraphic analysis of the lower Wilcox in general, and the Lake Creek field in particular, shows that the reservoir sandstones are depositionally equivalent to the fluvially influenced, seaward-stepping Ferron GS 2 Sandstone. In addition to stratigraphic analysis made possible by well logs, several cores from the Lake Creek field were available for permeability measurements. On the basis of well-log-based geologic mapping, well-log responses, and permeability measurements on Lake Creek core, we can compare the architecture and permeability structure of Ferron and lower Wilcox Group sandstones that were deposited in equivalent environments.

Important architectural similarities exist between the Cretaceous Ferron GS 2 Sandstone and the Tertiary lower Wilcox Lake Creek G-4 reservoir. In both cases the distributary-channel complex incises deeply into delta-front, delta-plain, and channel-mouth-bar facies (compare figs. 18, 29, and 34). The strata that encase the distributary-channel system are internally complex, unlike those in landward-stepping sandstones, such as the Ferron GS 5 (Fisher and others, 1993), where delta-front deposits are relatively homogeneous. Also, in both the Ferron GS 2 and the Lake Creek reservoir, mouth-bar sandstones are volumetrically important reservoir units. In contrast, mouth-bar facies are absent and delta-front sandstones are volumetrically less important in the landward-stepping Ferron GS 5 Sandstone.



QAa99c

Figure 34. Permeability profiles and geometric relations of distributary-channel, delta-front, and mouth-bar facies of the Lake Creek G-4 reservoir (after Grigsby and others, 1993).

Although the absolute permeability values differ between the Ferron outcrop and Lake Creek reservoir, there are important similarities in permeability relations within and between the two sandstones. We found two dominant macroforms in Ferron GS 2 distributary-channel sandstones, a lower cut-and-fill unit overlain by a low-to-high-sinuosity macroform. This architecture produced a characteristic vertical permeability profile (fig. 14). Analyses of well log data from the distributary-channel facies of the Lake Creek field G-4 reservoir show a similar vertical profile characterized by cycles of upward-increasing permeability (fig. 35). Furthermore, permeability profiles through channel-mouth-bar deposits from the Ferron GS 2 and the Lake Creek G-2 reservoir sand also show similar patterns (fig. 36).

One of our major conclusions from the extensive permeability study on the Ferron outcrop is that individual lithofacies must be considered the fundamental building blocks of sandstones and reservoirs. We reached this conclusion because of the stationarity of permeability statistics for individual lithofacies within a single genetic sequence and because the permeability distribution functions for lithofacies are simple, usually log-normal distributions, whereas cumulative permeability plots for facies typically have a complex shape. A plot of cumulative permeability of Lake Creek sandstones, grouped by facies, reveals irregularly shaped lines or curves for distributary-channel, channel-mouth-bar, and delta-front facies (fig. 37). These relations suggest that individual lithofacies also control permeability structure in this Wilcox reservoir, and that deep burial and cementation (Grigsby and others, 1993) have not obliterated the original permeability signature of the component lithofacies.

Finally, both Lake Creek and Ferron GS 2 Sandstones are quartz-rich and lithic arkoses, primarily cemented by quartz overgrowths (compare figs. 30 and 38). Thus, primary geologic controls on both sandstone composition and permeability have apparently survived burial and diagenesis in recognizable, predictable forms.

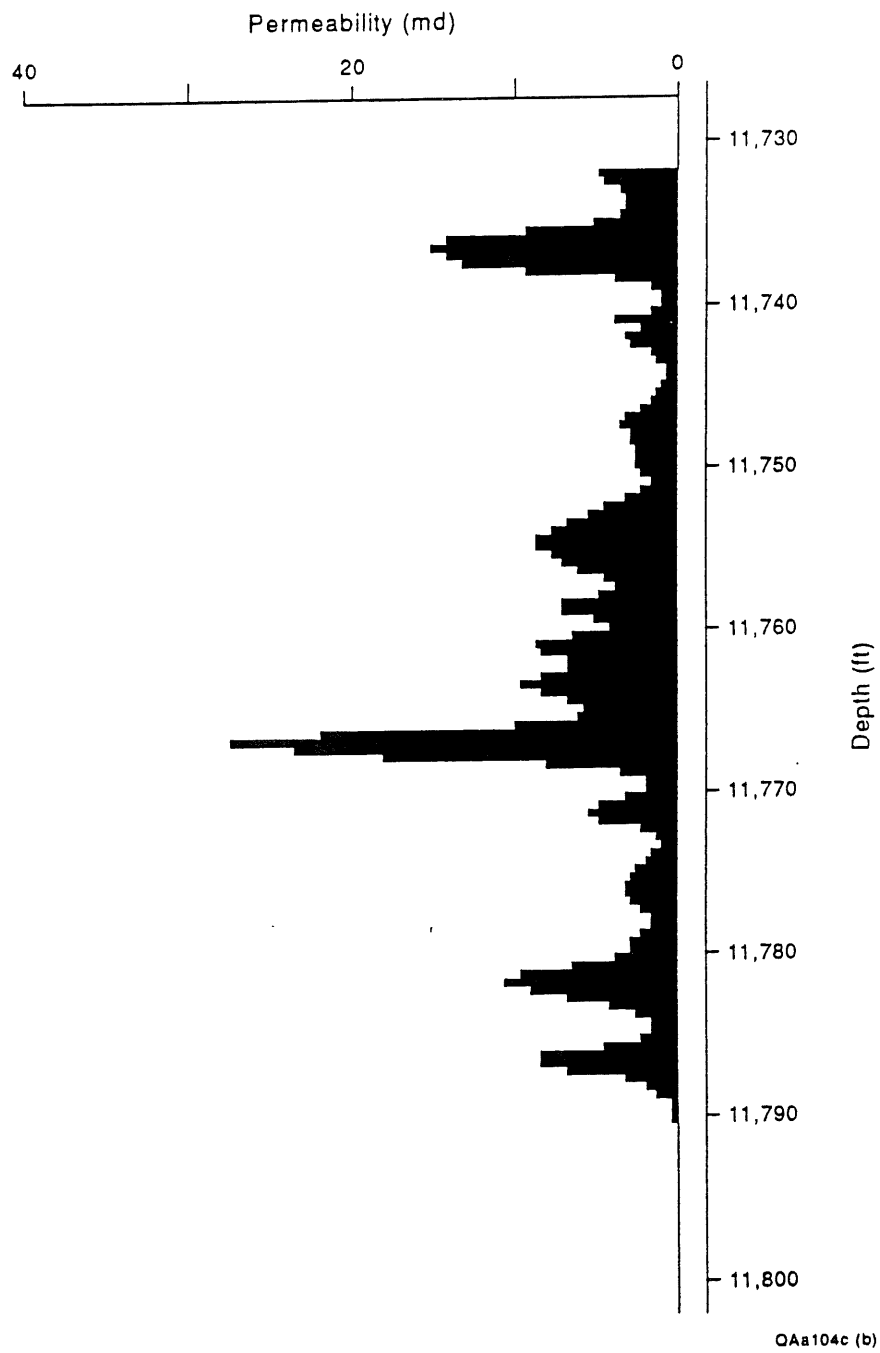
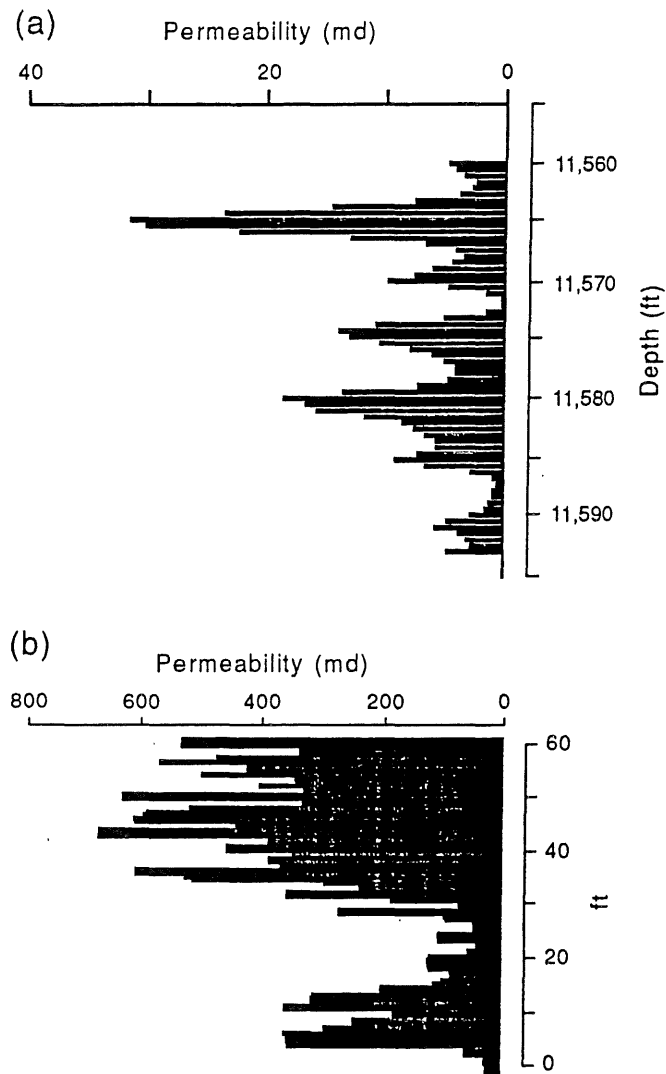


Figure 35. Vertical permeability profile from log data through the distributary-channel facies of the Lake Creek G-4 reservoir (after Grigsby and others, 1993).



QAa104(db)c

Figure 36. (a) Vertical permeability profile through a channel mouth bar of the Lake Creek G-2 reservoir. (b) Vertical permeability profile through the channel mouth bar facies of the Ferron GS 2 Sandstone (after Grigsby and others,



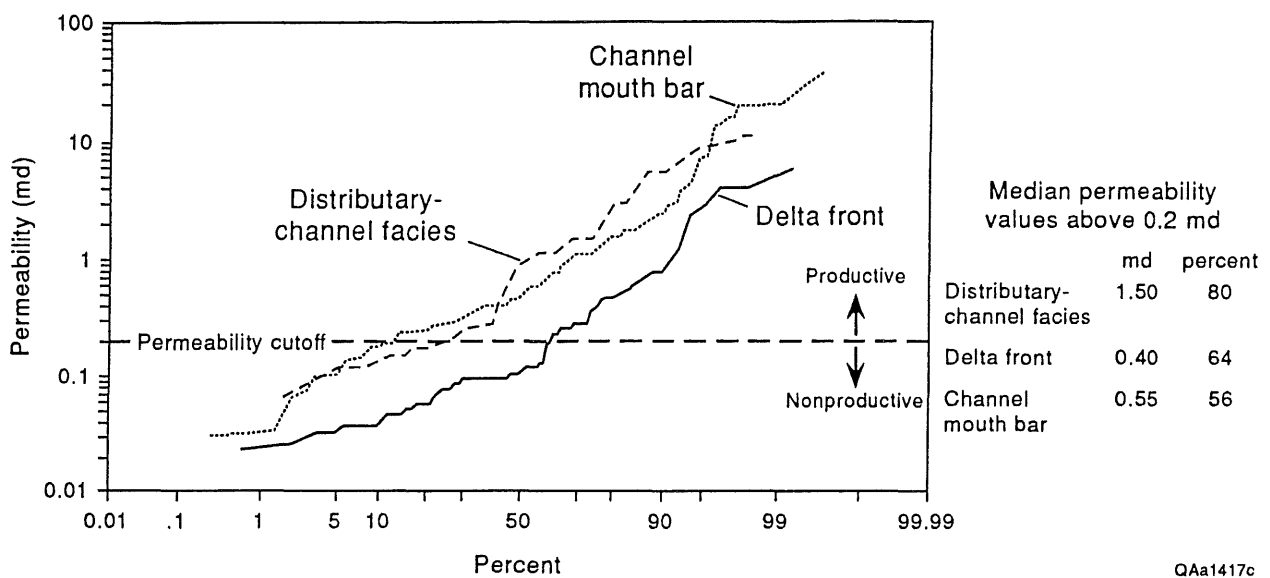


Figure 37. Cumulative frequency plot of channel mouth-bar; distributary-channel, and delta-front facies in Lake Creek field (after Grigsby and others, 1993).

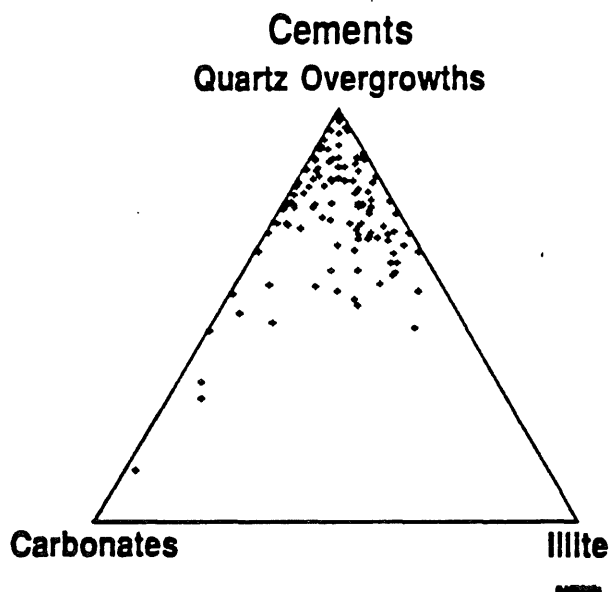
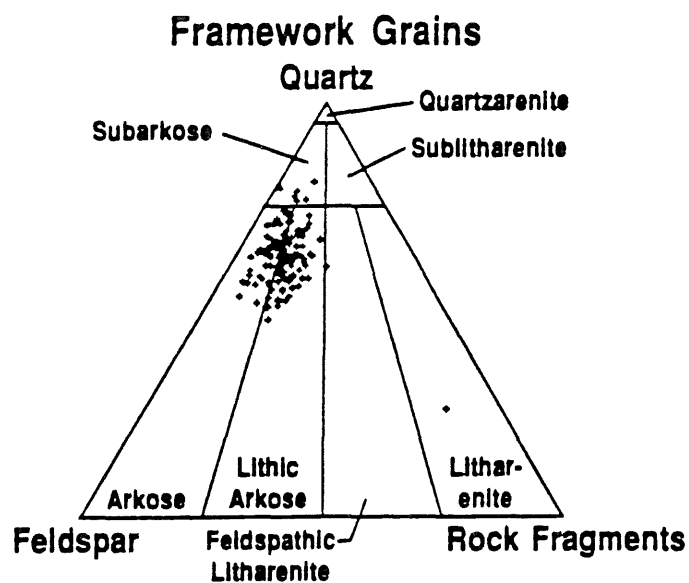


Figure 38. (a) Framework grain composition of Lake Creek G sandstones. (b) Cement composition of Lake Creek G sandstones (after Grigsby and others, 1993).

## SUMMARY AND CONCLUSIONS

We performed outcrop characterization studies of the seaward-stepping, fluvially dominated Ferron GS 2 deltaic sandstone to complement our companion investigation of the landward-stepping, wave-modified Ferron GS 5. These two sequences constitute the end members of the spectrum we find in Tertiary Gulf Coast natural gas reservoirs. By quantifying the architecture, composition, and permeability structure of these outcrops we will be able to better construct reservoir models, which in turn will permit improved evaluation of various drilling strategies to recover natural gas resources that previously would have been left in the ground at reservoir abandonment.

Distributary-channel complexes and the mouth-bar delta-front system are the major sand repositories in the seaward-stepping Ferron GS 2. Distributary-channel sandstones typically form amalgamated belts that consist of multiple-channel sand bodies. Because GS 2 was deposited during a time of active tectonic uplift of the source terrain and consequent relative sea-level fall, erosional truncation of older sands by younger deposits is common, diversity of preserved bedforms is low, and distributary-channel complexes form long, sinuous sandstone bodies. Air permeability measured on the outcrop ranges from less than 0.1 to more than 1,000 md. A plot of permeability versus cumulative frequency has a complex shape that reflects the presence of several permeability populations within the set of all distributary-channel sandstones. Subdividing the data set according to lithofacies type shows that individual lithofacies can be represented by a single permeability distribution. Therefore, lithofacies are the fundamental building blocks from which reservoir models should be assembled. As was the case for landward-stepping Ferron GS 5 distributary-channel sandstones, permeability correlation distances in GS 5 distributary-channel deposits are related to the dimensions of individual macroforms.

Permeability structure within the GS 2 distributary-channel facies is closely related to the nature of the channel fill. Five distinct lithofacies have an important influence on permeability variation. Trough crossbedded and horizontally bedded strata display the highest permeabilities

(10 to 1,000 md), ripple cross-strata and deposits associated with accretion and reactivation surfaces display the lowest permeabilities (0.1 to 10 md), and lag deposits have permeabilities that are intermediate between those two groups (1 to 100 md). The occurrence and distribution of these lithofacies are closely related to the two macroform types. The cut-and-fill macroform type is characterized by a thin lag deposit overlain by amalgamated trough cross strata. The low-sinuosity macroform is characterized by a succession of bed forms with well-developed accretion and reactivation surfaces. On the basis of permeability characteristics of lithofacies, cut-and-fill macroforms should display good connectivity between macroforms and good continuity within macroforms, whereas low-sinuosity macroforms should display moderate connectivity and poor continuity.

In contrast to the delta-front facies of GS 5, which is dominated by wave and storm processes, the delta-front and mouth-bar systems of GS 2 reflect the dominance of fluvial processes. Consequently, facies diversity is relatively high with a large proportion of preserved mud-rich lithologies. Overall progradation of the delta front is generally seaward and typically produces an upward-coarsening trend; prodelta, distal delta-front, bar-front, and proximal mouth-bar deposits are superposed during progradation. However, significant departures from this trend occur due to channel overextension and avulsion.

Distributary mouth-bar deposits are the primary locus of sand deposition and, along with associated bounding elements, display several significant scales of heterogeneity. At the largest scale, multiple mouth-bar sand bodies combine to form complexes that are 50 to 100 ft thick, one to several miles across, and several to ten miles in length. These complexes are separated from each other by thick, extensive interdistributary-bay deposits that range from less than a mile to several miles wide. Within the complex, individual mouth-bar sands sidelap one another and are highly compartmentalized by heterolithic bar-flank and fine-grained marsh and interdistributary-bay deposits. Internally, mouth-bar sands contain reactivation surfaces that may cause significant permeability discontinuities.

Advancement of mouth-bar deposits across the delta slope leads to gravitational instabilities and the generation of small- to medium-scale, sand-rich, slump and mass-flow structures. These units tend to be highly compartmentalized by prodelta, distal delta-front and bar-flank deposits.

Like distributary-channel deposits, permeability within the delta front displays a close relationship to lithofacies type. In addition, the occurrence and distribution of lithofacies shows a close correlation to facies type. On the basis of these relationships, wave-modified mouth-bar, proximal mouth-bar, and slump deposits should have very good to intermediate reservoir characteristics, while bar flank, distal delta-front, interdistributary-bay, and prodelta deposits should have poor to very poor reservoir characteristics.

Mineralogically, most distributary-channel sandstones are quartz-rich arkoses, whereas most mouth-bar and delta-front sandstones are subarkoses. Quartz overgrowths and kaolinite are the most abundant cementing agents, although the total volume of authigenic material is small. Ferron GS 2 sandstones show the same compositional relations as did the landward-stepping GS 5 sandstones, namely that reworking prior to final deposition reduces the amount of rock fragments and feldspars, producing a more mature rock mineralogically.

Using the field-scale distribution of distributary-channel and mouth-bar sandstones as a model to test the efficiency of infill drilling shows that seaward-stepping fluvial-deltaic sandstones are relatively simple targets. Because the mouth-bar system is areally extensive and good reservoir quality, drilling at 320-acre spacing essentially contacts more than 90 percent of the reservoir rock.

The seaward-stepping Ferron GS 2 is depositionally analogous to many fluvially influenced Tertiary Gulf Coast deltaic reservoirs. In particular, we find striking similarities between Ferron GS 2 and Wilcox Lake Creek reservoir sandstones. Both the Ferron GS 2 and the Lake Creek reservoir have complex delta-front mouth-bar systems that are deeply incised by distributary channels; permeability relations within the delta-front mouth-bar systems are similar for Lake Creek and Ferron-equivalent facies.

The results of this study support the initial hypotheses on which our outcrop characterization research was based, namely that outcrop studies can provide useful information regarding enhancement of natural gas recovery from known, mature reservoirs.

#### ACKNOWLEDGMENTS

This study was funded by the Gas Research Institute, contract number 5089-260-1902, and cofunded by the Department of

Energy, contract number DE-FG22-89BC-14403. We thank GRI Project Manager Anthony Gorody for his support and guidance throughout the project.

Summer field assistants Todd Muelhoeser, Chuck Cluck, and Sam Epstein helped with mapping and minipermeameter measurements. Field assistant Ted Angle contributed significantly to all aspects of the research throughout the three-year project. Discussions with Mike Gardner, Rex Cole, Rob Finley, Larry Lake, Mark Miller, Jon Holder, Dennis Nielson, and Lee Allison improved our understanding of the Ferron Sandstone, geostatistics, and petrophysics. We greatly appreciate the hospitality of the residents of Castle Valley, Utah.

This report was edited by Kitty Challstrom and prepared for publication by Susan Lloyd, Jamie H. Coggin, and Margaret L. Evans. Kerza A. Prewitt, Joel L. Lardon, and Tari Weaver drafted the figures, under the supervision of Richard L. Dillon, chief cartographer. Diane Spinney, Rick Edson, Rodney Heathcott, and Joseph Yeh helped with the various computer applications.

#### REFERENCES

- Allen, J. R. L., 1965, A review of the origin and characteristics of recent alluvial sediments: *Sedimentology*, v. 5, p. 89-191.
- Armstrong, R. L., 1968, Sevier orogenic belt in Nevada and Utah: *Geological Society of America Bulletin*, v. 79, p. 429-458.

- Dreyer T. A., Scheie, A., and Walderhaug, O., 1990, Minipermeameter-based study of permeability trends in channel sand bodies: American Association of Petroleum Geologists Bulletin, v. 74, no. 4, p. 359–374.
- Elliot, T., 1986, Siliciclastic shorelines, *in* Reading, H. G., ed., Sedimentary environments and facies, 2d ed.: Palo Alto, California, Blackwell Scientific Publications, p. 155–188.
- Fisher, R. S., Barton, M. D., and Tyler, Noel, 1993, Architecture, composition, and permeability structure of a landward-stepping fluvial-deltaic sequence, Ferron Sandstone (Cretaceous), central Utah: draft contract report submitted to GRI, in preparation.
- Folk, R. L., 1974, Petrology of sedimentary rocks: Austin, Texas, Hemphill Publishing Company, 182 p.
- Friend, P. F., 1983, Towards a field classification of alluvial architecture or sequence: Sedimentology, v. 6, p. 345–354.
- Gardner, M. H., 1991, Sequence stratigraphy of the Ferron Sandstone, east-central Utah, *in* Tyler, Noel, Barton, M. D., and Fisher, R. S., eds., Architecture and permeability structure of fluvial-deltaic sandstones: a field guide to selected outcrops of the Ferron Sandstone, east-central Utah: The University of Texas at Austin, Bureau of Economic Geology, guidebook prepared for 1991 field trips, p. 4–55.
- Gardner, M. H., 1993, Sequence stratigraphy of Cretaceous strata, central Utah: Colorado School of Mines, Ph.D. dissertation, in preparation.
- Goggin, D. J., 1988, Geologically sensible modeling of the spatial distribution of permeability in eolian deposits, Page Sandstone (Jurassic), northern Arizona: The University of Texas at Austin, Ph.D. dissertation, 418 p.

- Grigsby, J. D., Guevara, Edgar, Levey, R. A., Sippel, M. A., Howard, W. E., Vidal, J. M., and Ballard, James, 1992, Secondary natural gas recovery: targeted technology applications for infield reserve growth in deltaic sand-rich, low- to conventional-permeability reservoirs in the Wilcox Group, Lake Creek field, Texas: draft topical report submitted to the Gas Research Institute, 105 p.
- Haldorsen, H. H., and Lake, L. W., 1984, A new approach to shale management in field-scale models: Society of Petroleum Engineers Journal, v. 24, p. 447–457.
- Hunter, R. E., and Clifton, H. E., 1982, Cyclic deposits and hummocky cross stratification of probable storm origin in Upper Cretaceous rocks of the Cape Sebastian area, southwestern Oregon: Journal of Sedimentary Petrology, v. 52, no. 1, p. 127–143.
- Jackson, R. G., II, 1976, Depositional model of point bars in the lower Wabash River: Journal of Sedimentary Geology, v. 46, p. 579–594.
- Kittridge, M. G., 1988, Analysis of permeability variation—San Andres Formation (Guadalupian) Algerita Escarpment, Otero County, New Mexico: The University of Texas at Austin, Master's thesis, 361 p.
- Kittridge, M. G., Lake, L. W., Lucia, F. J., and Fogg, G. E., 1989, Outcrop-subsurface comparisons of heterogeneity in the San Andres Formation: Society of Petroleum Engineers paper, SPE 19596, p. 259–273.
- Koning, H. L., 1982, On an explanation of marine flow in sand, *in* Saxov, S., and Nieuwenhuis, J. K., eds., Marine slides and other mass movements: New York, Plenum Press, p. 83–94.
- Miall, A. D., 1985, Architectural-element analysis, a new method of facies analysis applied to fluvial deposits: Earth-Science Reviews, v. 22, p. 261–308.



- Miller, M. A., Holder, Jon, and Gray, K. E., 1993, Petrophysical property measurements and scale-up transforms, Ferron Sandstones, Central Utah, in preparation.
- Nemec, W., Steel, R. J., Gjølberg, J., Collinson, J. D., Prestholm, E., and Oxnevad, I. E., 1988, Anatomy of a collapsed and reestablished delta front in Lower Cretaceous of eastern Spitzbergen: gravity sliding and sedimentation processes: American Association of Petroleum Geologists Bulletin, v. 72, no. 4, p. 454–476.
- Ryer, T. A., 1981a, Deltaic coals of the Ferron Sandstone Member of the Mancos Shale predictive model for Cretaceous coal-bearing strata of the western interior: American Association of Petroleum Geologists Bulletin, v. 65, no. 11, p. 2323–2340.
- \_\_\_\_\_ 1981b, The Muddy and Quitcupah projects: a project report with descriptions of cores of the I, J, and C coals beds from the Emery coal field, central Utah: U.S. Geological Survey Open-File Report 81-460, 34 p.
- \_\_\_\_\_ 1982, Possible eustatic control on the location of Utah Cretaceous coal fields: Utah Geological and Mineralogical Survey, Bulletin 118, Proceedings, 5th ROMOCO Symposium, p. 89–93.
- \_\_\_\_\_ 1983, Transgressive-regressive cycles and the occurrence of coal in some Upper Cretaceous strata of Utah: Geology, v. 111, p. 207–210.
- Schmidt, Volkmar, and MacDonald, D. A., 1979, Texture and recognition of secondary porosity in sandstones, *in* Scholle, P. A., and Schluger, P. R., eds., Aspects of diagenesis: Society of Economic Paleontologists and Mineralogists Special Publication No. 26, p. 209–226.
- Stalkup, F. I., and Ebanks, W. J., Jr., 1986, Permeability variation in a sandstone barrier island-tidal delta complex, Ferron Sandstone (Lower Cretaceous), central Utah: Society of Petroleum Engineers paper, SPE 15532, p. 1–8.

- Swift, D. P., 1968, Coastal erosion and transgressive stratigraphy: *Journal of Geology*, v. 76, p. 444–456.
- Tomutsa, L., Jackson, S. R., Szpakiewicz, M., 1986, Geostatistical characterization and comparison of outcrop and subsurface facies: Shannon shelf sand ridges: Society of Petroleum Engineers paper, SPE 15127, p. 317-322.
- van Veen, F. R., 1977, Prediction of permeability trends for water injection in a channel-type reservoir, Lake Maracaibo, Venezuela: Denver, Society of Petroleum Engineers 52nd Annual Fall Technical Conference, October 9–12, SPE paper 6703.
- Weber, K. J., 1982, Influence of common sedimentary structures on fluid flow in reservoir models: *Journal of Petroleum Technology*, March, p. 665–672.
- \_\_\_\_\_ 1986, How heterogeneity affects oil recovery, *in* Lake, L. W., and Carroll, H. B., eds., *Reservoir characterization*: Orlando, Academic Press, p. 487–544.